uOttawa

L'Université canadienne
Canada's university

FACULTÉ DES ÉTUDES SUPÉRIEURES ET POSTOCTORALES

uOttawa

L'Université canadienne
Canada's university

FACULTY OF GRADUATE AND POSDOCTORAL STUDIES

Cynthia Moffat
AUTEUR DE LA THÈSE / AUTHOR OF THESIS

M.Sc. (Biochemistry)
GRADE / DEGREE

Department of Biochemistry, Microbiology and Immunology
FACULTÉ, ÉCOLE, DÉPARTEMENT / FACULTY, SCHOOL, DEPARTMENT

Impact of the AMPK γ2 R302Q Mutation on Human Skeletal Muscle Metabolism
TITRE DE LA THÈSE / TITLE OF THESIS

Mary-Ellen Harper
DIRECTEUR (DIRECTRICE) DE LA THÈSE / THESIS SUPERVISOR

CO-DIRECTEUR (CO-DIRECTRICE) DE LA THÈSE / THESIS CO-SUPERVISOR

Thomas Moon

Jean-Marc Renaud

Gary W. Slater
Le Doyen de la Faculté des études supérieures et postdoctorales / Dean of the Faculty of Graduate and Postdoctoral Studies

Impact of the AMPK γ2 R302Q Mutation on Human Skeletal Muscle Metabolism

M. Sc. Thesis of Cynthia Moffat

Supervisor: Mary Ellen Harper, Ph. D.

A thesis submitted to the Faculty of Graduate and

Postdoctoral Studies in partial fulfilment of the

requirements for the degree of Masters of Science, Biochemistry

Faculty of Medicine

Department of Biochemistry, Microbiology and Immunology

University of Ottawa

Ottawa, ON, Canada

Your file Votre référence
ISBN: 978-0-494-73837-5
Our file Notre référence
ISBN: 978-0-494-73837-5

Abstract

AMP-activated protein kinase, AMPK, is a heterotrimeric protein complex comprised of an α catalytic, and of β and γ regulatory subunits. It is widely conserved across most organisms and is commonly referred to as the master regulator of cellular metabolism. By responding to increases in the AMP:ATP ratio, AMPK promotes ATP producing catabolic pathways, while simultaneously inhibiting ATP consuming anabolic pathways. Naturally occurring mutations in AMPK exist in various organisms and these can have a severe impact on fuel storage and metabolism. One such mutation in humans is the R302Q mutation in the γ2 subunit; the outcome is accelerated glycogen production and impaired electrical conductance within the heart, resulting in Wolff-Parkinson White (WPW) syndrome. The impact of this rare mutation on AMPK activity is not well understood. By examining skeletal muscle samples from affected patients from the Ottawa region, we strove to determine the impact of the R302Q mutation on AMPK activity, and skeletal muscle metabolism. Skeletal muscle biopsies were utilized for histological analyses and cell culture determinations of fuel storage and AMPK activity. Trends for decreased triglyceride storage and increased glycogen storage, as well as impaired basal and AMP-stimulated AMPK activity were observed in the affected patient populations. Corollary work done in an adenoviral infected C2C12 muscle cell line expressing human γ2 WT or the R302Q variant yielded no difference between groups in fuel storage or protein phosphorylation due to limitations (infection efficiency) of this model.

Acknowledgments

I would like to take this opportunity to thank all those who have been instrumental in helping me complete my M.Sc. degree at the University of Ottawa

- Thank you Dr. Mary Ellen Harper for all your support, guidance and the occasional pep talk. You have been an amazing supervisor, always positive and easy to talk to. You took a risk letting me work in the lab just after my first year of University, but without all the great experiences I obtained within those 3 summers, I probably wouldn't even be here today. I will never forget all you've taught me and given me during my time working with you.

- Thank you Mahmoud Salkhordeh, Jian Xuan and Linda Jui for all the expert technical assistance you provided.

- Thank you to all the former and current lab members. You brightened every day and provided invaluable assistance and advice with my ongoing work. I would especially like to thank Dr. Celine Aguer and Dr. Erin Seifert for all your guidance and counsel throughout my studies, and Carmen Estey for your constant support and the occasional well needed coffee break. I will always look back on my time in the lab fondly thanks to all of you. I'm certain these friendships will last a lifetime.

- Thank you to everyone who assisted me in conducting my experiments. I would particularly like to thank Stephanie Thorn for her assistance in the SAMS peptide assay. I couldn't have done it without you.

- Thank you to my family and friends for supporting me and tolerating me when experiments weren't working as I had hoped. Without you to help ground me, I could not have completed all I have within the past 3 years.

Table of Contents

List of Abbreviations

A

Ab-beads	Antibody Conjugated Immunoprecipitation Beads
ACC	Acetyl-CoA Carboxylase
Adv	Adenoviral Vector
AICAR	5-aminoimidazole-4-carboxamide-1-β -d-ribofuranoside
AIS	Autoinhibitory Sequence
Akt	Protein Kinase B (PKB)
AMP	Adenosine-5`-monophosphate
AMPK	AMP Activated Protein Kinase
AMPKK	AMPK Kinase
AS160	Akt Substrate 160
Asp	Aspartate
ATP	Adenosine-5`-triphosphate
a.u.	Arbitrary Units

B

BCA	Bicinchonic Acid
BMI	Body Mass Index
BSA	Bovine Serum Albumin

C

C2GM	C2C12 Growth Media
C2DM	C2C12 Differentiation Media
CAMK	Ca^{2+}/Calmodulin Dependent Protein Kinase
CaMKK	CAMK Kinase
CBM	Carbohydrate Binding Motif
CBS	Cystathione Beta Sheets
CD56	Cluster of Differentiation 56

D

DM	Human Myoblast Differentiation Medium
DMEM	Dulbecco's Modified Eagle Medium
DNP	Dinitrophenol

E

ECG	Electrocardiogram
ECL	Enhanced Chemiluminescence
Elm1	Elongated Morphology 1

F

FAT/CD36	Fatty Acid Translocase/Cluster of Differentiation 36

FDG	18F-Fludeoxy Glucose
G	
G1P	Glucose-1-phosphate
G6P	Glucose-6-phosphate
GFP	Green Fluorescent Protein
GM	Human Myoblast Growth Medium
GS	Glycogen Synthase
GP	Glycogen Phosphorylase
H	
h	Hour(s)
HMGR	3-hydroxy-3-methyl-glutaryl-CoA Reductase
I	
IMCL	Intramyocellular Lipid Content
IP	Immunoprecipitation
L	
LKB1	Serine/Threonine Kinase 11
M	
MARK2	MAP/Microtubule Affinity-Regulating Kinase 2
MCD	Malonyl-CoA Decarboxylase
min	Minute(s)
MO25	Mouse Protein 25
MOI	Multiplicity of Infection
mTORC	Mammalian Target of Rapamycin Complex
N	
NADH	Nicotinamide Adenine Dinucleotide Hydride
NADPH	Nicotinamide Adenine Dinucleotide Phosphate Hydride
O	
O.C.T.	Optical Cutting Temperature
P	
p-(protein)	Phosphorylated (Protein)
Pak1	Snf1 Associated Kinase 1
PAS	Periodic Acid Schiff
PBS(-AG)	Phosphate Buffered Saline (Supplemented with Antibiotic-Antimycotic and Gentamycin)
PEG	Polyethylene Glycol
PET	Positron Emission Tomography
PGC-1α	PPARγ Coactivator 1α
PMSF	Phenyl-Methyl-Sulfonyl Fluoride

PP2A/C	Protein Phosphatase 2A/2C
PPARγ	Peroxisome Proliferator Associated Receptor γ
PS	Pseudosubstrate
R	
R225Q	Glutamine Substitution for Arginine-225
R225W	Tryptophan Substitution for Arginine-225
R302Q	Glutamine Substitution for Arginine-302
RIPA	Radioimmunoprecipitation Assay Buffer
RN^-	Rendement Napole
S	
SDS-PAGE	Sodium Dodecyl Sulphate – Polyacrylamide Gel Electrophoresis
SEM	Standard Error of the Mean
Snf1	Sucrose Non-Fermenting 1
SREBP1c	Sterol Response Element Binding Protein-1c
STRAD	STE20 Related Adaptor
T	
T400N	Asparagine Substituion for Threonine 400
TAB1/2/3	Tak1 Associated Binding Protein 1/2/3
Tak1	TGFβ-Activated Kinase 1
TBC1D1	tre-2/USP6 BUB2, cdc16 Domain Family Member 1
TE	0.25% Trypsin-EDTA Buffer
Thr-172	Threonine-172
TNFα	Tumour Necrosis Factor α
TG	Triglyceride Content
TGFβ	Transforming Growth Factor β
TSC1/2	Tuberous Sclerosis Protein 1/2
Tos3	Target of Sbf 3
V	
v/v	Volume per Volume
v:v	Volume to Volume
W	
w/v	Weight per Volume
WHO	World Health Organization
WPW	Wolff-Parkinson White Syndrome
WT	Wild Type
Z	
ZMP	5-aminoimidazole-4-carboxamide-1-D-ribofuranosyl-5'-monophosphate

List of Figures

List of Tables

Introduction

AMP-activated protein kinase (AMPK) is a heterotrimeric protein comprised of an α catalytic, and of β and γ regulatory subunits. It is widely conserved across many organisms – from yeast to humans, and is commonly referred to as the master fuel regulator of the cell. Through the action of its γ subunit it can rapidly respond to changes in the AMP:ATP ratio within the cell to restore the energy balance during times of high energy demand. At the cellular level AMPK promotes ATP producing catabolic pathways, while simultaneously inhibiting ATP consuming anabolic pathways. At the organismal level, through its activity within the hypothalamus, it can modulate feeding behaviour and satiety signals thereby regulating whole body energy stores.

Structural Aspects

Each subunit exists in various isoforms encoded by unique genes, with varied expression throughout the different tissues within the body. Each subunit plays its own unique and important role in AMPK activation and regulation. Structural elements of the various isoforms are summarized in Figure 1.

Recent crystal structure determinations of AMPK have allowed greater insight into the relationships between the various subunits. The αβγ core complex was crystallized in 2007 and represents the COOH terminal regions of the α and β subunits, and the complete γ1 subunit (131). Other crystal structures of the yeast homolog sucrose non-fermenting protein 1 (Snf1) and its regulatory subunits as well as the solo

Figure 1. AMPK Subunits. A) Various α, β and γAMPK subunits and isoforms with important domains highlighted: Kinase domain, autoinhibitory sequence (AIS), subunit binding domain (SBD), carbohydrate binding motif (CBM), cystathione beta sheet (CBS) regions (1-4). B) Representation of subunit interaction and complex formation.

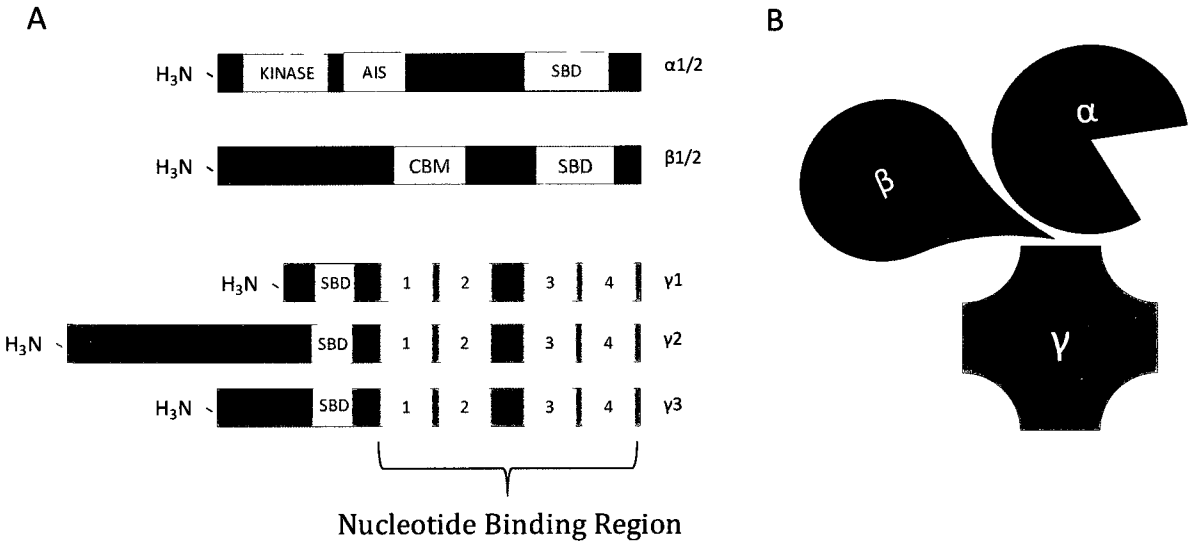
A
H3N
KINASE
AIS
SBD
α1/2
H3N
CBM
SBD
β1/2
H3N
SBD
1
2
3
4
γ1
H3N
SBD
1
2
3
4
γ2
H3N
SBD
1
2
3
4
γ3
Nucleotide Binding Region
B
α
β
γ

α1 subunit have shed additional light on the intricate structure of the AMPK monomer (92, 107).

The α subunit contains the kinase domain, which is crucial to AMPK activity. It exists in two isoforms – α1 and α2. Both isoforms are highly similar, each with approximately 550 residues, and a highly conserved NH_2 terminal domain. Structurally, the α subunit belongs to the Ca^{2+}/calmodulin dependent protein kinase (CAMK) branch of the kinome, whose related proteins are all activated by serine/threonine kinase 11 (LKB1). α1 is widely expressed, with protein evident in the heart, liver, kidney, brain, spleen, lungs as well as skeletal muscle (123). α2 is more conservative in its tissue distribution, being strongly expressed in skeletal muscle and to a lesser degree in the heart, liver, brain, and kidney (123). Beyond the kinase domain, the α subunit contains a subunit interacting domain, that contacts the β subunit (33, 61). From the crystal structures of this subunit, we know that the subunit interacting domain is the backbone of the protein, and that it is a helix-loop-helix regulatory sequence overlapping with the γ subunit (131). Within the cell the two isoforms are differentially compartmentalized. The α1 subunit is distributed evenly throughout the cytosol, whereas the α2 is localized to the nucleus in times of energy demand (112). This disparity in distribution suggests a specialized role for different complexes in cellular regulation, with α1-containing complexes functioning to control signalling pathways, while α2-containing complexes regulate transcription and gene expression.

Along with the integral kinase domain, the α subunit also contains the crucial threonine residue for which phosphorylation is required during protein activation – a

feature common in all kinases within the CAMK branch of the kinome (56). Phosphorylation of Thr-172 of the α subunit results in as great as a 1000-fold increase in enzyme activity, and is a key activation step in response to changes within the cell (128). It has also been shown that the α subunit also contains an autoinhibitory sequence (AIS) (33). AIS is a feature common to the kinase family to which the α subunit belongs. Suspicions were first aroused with the observation that a truncated α subunit was capable of activity in the absence of either the β or γ subunits (33). The AIS was uncovered by examining structural homology to the MAP/microtubule affinity-regulating kinase 2 (MARK2), a close relative of AMPK (63). Indeed a 3 helix loop structure was found to exist by the small lobe of the kinase domain. This structure, in other AMPK related kinases, corresponds to the ubiquitin-associated domain, and was known to be important in the LKB1 phosphorylation process (63). Further studies into the function of the AIS revealed that point mutations of key residues within the three helix loop region result in a constitutively active AMPK (98).

The β subunit exists in two highly similar isoforms, β1 and β2 which only differ in the first 65 of 270 residues. Notably, while the β1 subunit has almost the same widespread distribution as the α1 subunit, the β2 subunit is only expressed in skeletal muscle and, to a lesser extent, the heart (26). The β subunit also has two main domains, the glycogen binding domain (GBD) (recently reclassified as a carbohydrate binding motif (CBM)) in the middle of the peptide, and the subunit binding sequence at the COOH terminal end that interacts with both the α and γ subunits. Also contained within the β subunit is a potential myristolation site within the CBM which may anchor the complex to membranes (60, 85, 101). The CBM was first shown to bind glycogen

with the development of the crystal structure – a β-cyclodextrin molecule was shown bound to the then GBD domain (7, 102). Initial studies sought to elucidate a role for glycogen in AMPK activation; however, *in vitro* measurements of AMPK activity revealed no impact of glycogen on basal or activated activity. *In vivo* studies, on the other hand, have demonstrated that increased glycogen stores within muscle cells contributes to an inhibition of AMPK activation, even in response to exercise or chemical activators (137, 145). In 2003, one research group demonstrated an association of fluorescently tagged AMPK with glycogen and glycogen synthase (GS) (60). Somewhat surprisingly, AMPK was not associated with the stable isolated glycogen α-particles, as had been expected (100). In fact, AMPK associated only with the highly dynamic regions of glycogen cycling, binding almost exclusively to the branched α1-6 linkages of degraded glycogen, as opposed to the α1-4 linkages within the glycogen structure (73). In agreement, addition of α1-6 linked glycogen to an *in vitro* AMPK activity assay successfully inhibited AMPK activation, but required the presence of an intact CBM (73, 81). This remarkable association and control adds another dimension of AMPK-mediated energy maintenance, as these results demonstrate AMPK acts not only as an AMP:ATP energy sensor, but also a sensor of stored fuel levels.

The γ subunit is perhaps the most important subunit within the AMPK complex as it is solely responsible for the enzyme's ability to sense AMP:ATP levels within the cell. The γ isoforms are the most highly variable, existing in three unique forms – γ1, γ2, and γ3. The mostly widely expressed γ isoform is γ1; it is the smallest at 331 residues and is expressed in almost every cell type and tissue within the body (79).

The γ3 subunit is the next largest γ isoform at 489 residues, and is the most restricted in its tissue expression, only being found in skeletal muscle, and there only in glycolytic-oxidative type 2a fibers (79, 151). The γ2 subunit is by far the largest isoform at 569 residues, though there does exist a splice variant that is only 328 residues. Its expression is limited to the heart, brain, placenta and skeletal muscle (28). Its most important role is in the heart where it regulates cardiac AMPK activity.

All of the γ subunits have highly conserved COOH terminal domains while their NH_2 termini are highly variable in both length and sequence (131). Not surprisingly, the conserved COOH region contains the indispensible nucleotide binding domain. Initially it was thought that ADP was responsible for AMPK activation (20, 93). Early *in vitro* studies confirmed this, until it was realized the ADP preparations were less pure than initially assumed. Stringent purification revealed that contaminating AMP was actually responsible for the apparent ADP activation effect (37). Further studies revealed that the AMPK enzyme binds both ATP and AMP competitively with a stoichiometry of 2 nucleotides per molecule (116). Sequence analysis indentified the presence of 4 cystathione β-sheet (CBS) repeats that together fold into 2 Bateman domains, each capable of binding 2 nucleotides (7, 131, 148). The x-ray crystal structure of AMPK was subsequently able to shed more light onto the function of these domains.

In general, each CBS domain possesses a helix-loop-strand structure, with the nucleotides binding in a hydrophobic pocket by hydrogen bonding with the peptide backbone (131, 148). The adenyl group is anchored into place by a conserved Asp residue in 3 of the 4 pockets (148). The phosphate group points into the protein in a

solvent accessible core. These structural characteristics result in a high degree of connectivity between the nucleotides and the protein. However, the four CBS domains are not identical. CBS 1 and 3 both bind AMP or ATP interchangeably and are therefore the main contenders in AMPK activation in response to altered cellular fuel levels (148). CBS4 binds AMP securely, unable to interchange with ATP to act as an energy sensor (131, 148). The CBS2 domain binds no nucleotide, lacking the required Asp residue (131). It does, however, still play an important role in AMPK activity. A pseudosubstrate sequence (PS) is found within the CBS2 pocket that contains the consensus sequence for acetyl-CoA carboxylase (ACC) phosphorylation (117). In the absence of AMP the PS can associate with the substrate binding domain of the α subunit, blocking activity. With AMP bound, the γ subunit undergoes a conformational change that deforms the CBS2 domain, bringing the PS out of contact with the active site of the α subunit (117). This was confirmed with a point mutation in the PS (V153S) which resulted in autophosphorylation of the PS, thus verifying its contact with the active site in the absence of AMP (117).

An active AMPK molecule contains one of each of the three subunits. Expression of the various isoforms dictates which complexes will be most common. Within the heart the α2β2γ2 complex is the most abundant, whereas in skeletal muscle the α2β2γ3 complex dominates (26). As each isoform varies from its sibling forms, the complement of isoforms present in a complex can impact the role and response of AMPK within the cell.

Functional Analyses of AMPK in Yeast

Sequence analysis revealed a strong similarity between the mammalian α catalytic subunit of AMPK and the yeast protein Snf1 (86, 147). Snf1 is required for yeast growth on non-glucose carbon sources, which are more challenging to catabolize (25). Yeast with a ΔSnf1 genotype are incapable of growing on non-glucose carbon sources. Snf1 activity works to turn on genes required for sucrose and other carbon source metabolism (103). It also works to regulate fatty acid metabolism, and carbohydrate storage (147). Snf1 is activated during glucose depletion, specifically through the phosphorylation of Thr-210 on Snf1; it is directly inhibited by glucose (88). It exists as part of a heterotrimeric complex, with the Snf1 protein containing the kinase domain. Bound to Snf1 is either galactose metabolism protein 83 (Gal83), Snf1 interacting protein 2 (Sip2), or Sip1 (88). The former two are able to bind glycogen and respond to changes in glucose levels within the cell, much like the AMPK β subunit. Each of these Snf1-binding proteins controls localization within the cell as well as interactions with substrates. Gal83 is the main protein bound to Snf1, and is the first responder to glucose deprivation (88). Lastly, Snf4 binds to the Snf1 complex, and is required for Snf1 activity. Like the AMPK γ subunit, it contains 4 CBS repeats, however it is still unclear if it binds nucleotides. One crystal structure was created in the presence of AMP, but none were bound, whereas a second crystal did show bound AMP (65). Even though AMP has not been shown to activate it *in vitro* (86, 141), mutations created within the CBS domains, that resemble human mutations, affect Snf1 activation and phosphorylation – a tantalizing observation that suggests a role for AMP binding in Snf1 activation (88).

Three upstream kinases of Snf1 were identified in yeast, Elm1, Pak1, and Tos3 all work to phosphorylate Thr-210 on Snf1, which is a requirement of activation (88). There is a great deal of redundancy in their contributions to overall activity, as only a triple ΔElm1, ΔPak1, ΔTos3 deletion can emulate the ΔSnf1 phenotype (59, 88). The identification of these three kinases was a boon to the study of AMPK function as it contributed substantially to the discovery of new AMPK kinases (AMPKKs).

Activation of AMPK

In 1968, Atkinson proposed the 'Adenylate Charge' hypothesis. He postulated that for energetically driven reactions to proceed, the pools of ATP and ADP must remain relatively constant in relation to each other, as they are, ostensibly, the only two relevant metabolites (10). The cell would therefore strive to maintain the balance of key metabolites. Adenyl kinase was identified to be of clear importance in sensing demand for ATP, by using 2 ADP molecules from a growing pool to create one new strongly energetic ATP and one left over AMP molecule. As such, as the cell depletes its energy reserves, and endeavours to preserve its ATP and ADP pools, a marked increase in the levels of AMP, relative to ATP, will occur. It was also observed that ATP depletion leads to a rapid surge in ATP production, such that ATP exhaustion and synthesis were balanced to restore cellular ratios of ATP, ADP and AMP. There was speculation into how this tight control was achieved, and it took many years for the master regulator, AMPK, to be revealed.

Research into upstream kinases of ACC and 3-hydroxy-3-methyl-glutaryl-CoA reductase (HMGR), two proteins which are essentially the rate limiting enzymes for hepatic fatty acid and cholesterol synthesis, respectively, revealed what was later

determined to be AMPK (14, 24). This new kinase was discovered to be activated by AMP, which made it a strong contender for the key player in adenylate charge balance (150). A number of studies conducted in the 1980s, unequivocally demonstrated that the two kinases were one and the same, and the name AMP-activated protein kinase (AMPK) was appropriately ascribed (22, 90).

Figure 2 summarizes various contributors to AMPK regulation. AMPK, as detailed above, binds interchangeably to either AMP or ATP within the γ subunit. As the AMP:ATP ratio increases, AMP preferentially binds to the CBS domains of the γ subunit causing an allosteric activation of the kinase domain within the α subunit (116). This slight conformational change can result in a moderate increase in AMPK activity alone, the intensity of which depends on the γ isoform present. The γ1 isoform results in a larger AMP only response, with an increase in activity up to 3-fold, whereas the γ2 isoform only exhibits a 2-fold increase in activity (77).

Like other kinases within the CaMK branch of the kinome, AMPK requires phosphorylation for activation. Within the α subunit, phosphorylation at Thr172 results in an additional 10 fold increase in AMPK activity within the cell (56). Under conditions resulting in a high AMP:ATP ratio phosphorylation of the α subunit is increased. Initially this was thought to be due to a conformational change that made it a more desirable substrate for upstream kinases (57). However, it was later determined that AMP binding within the γ subunit results in the α subunit retaining its phosphate group for a longer period, and mitigating its deactivation by phosphatases (113). This suggested that the AMPK complex is constantly being phosphorylated and dephosphorylated in the absence of AMP. While this may seem futile, theoretically it

Figure 2. Summary of Various AMPK Activators and Inhibitors. AMPK upstream kinases (serine/threonine kinase 11 (LKB1), transforming growth factor-β activated kinase 1 (Tak1), and Ca^{2+}/calmodulin activated kinase kinase (CaMKK)) activate AMPK through interaction and phosphorylation of the α subunit. Protein phosphatases 2A/C (PP2A/C)inhibit AMPK activity through dephosphorylation of the α subunit. Glycogen can bind the β subunit resulting in inhibition. Small molecular activators such as AICAR/ZMP and AMP act directly on the γ subunit. Indirect activators (metformin, dinitrophenol (DNP) and rotenone) work by increasing the AMP:ATP ratio, while Compound C can work to inhibit activation by AICAR.

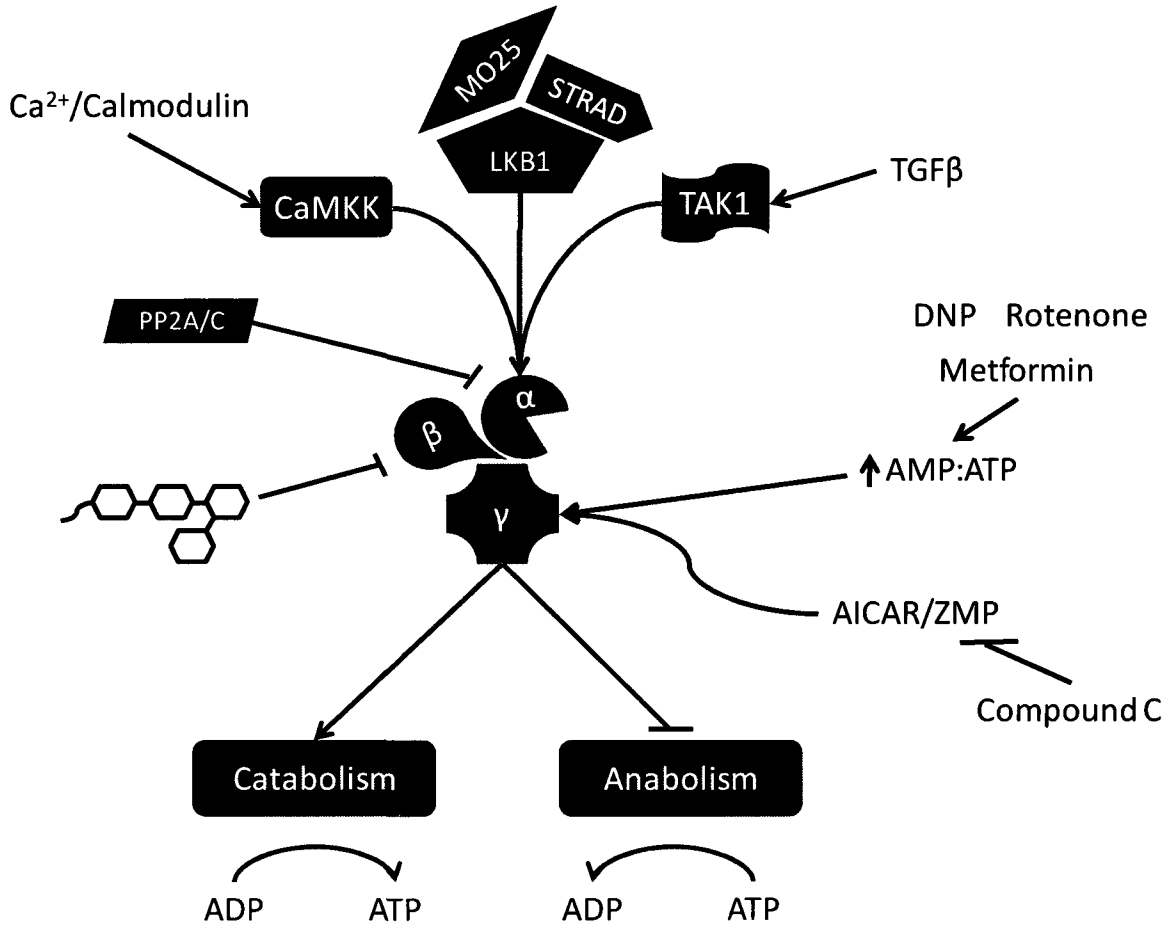
Ca2+/Calmodulin
MO25
STRAD
LKB1
CaMKK
TAK1
TGFβ
PP2A/C
DNP
Rotenone
Metformin
α
β
γ
AMP:ATP
AICAR/ZMP
Compound C
Catabolism
Anabolism
ADP
ATP
ADP
ATP

would allow AMPK to respond extremely rapidly to changes in energy stores within the cell.

Widely accepted as the main AMPKK within the cell, LKB1 was also the first enzyme discovered to phosphorylate and activate AMPK (55). LKB1 was already known to researchers investigating cancer cell development. Mutations in LKB1 are known to lead to Peutz-Jeghers syndrome, a condition characterized by growth of polyps in the intenstine, pigmented macules on the skin and other neoplasms (120, 138). In 2003, a crude purification of AMPK from rat liver included associated LKB1, implicating it as a possible activator of AMPK. LKB1 exists in a heterotrimeric complex with STE20 related adaptor (STRAD) and mouse protein 25 (MO25) (55). When in complex, LKB1 appears to be constitutively active, to our knowledge there are no studies indicating any changes in LKB1 activity in response to any stimulus (110). Due to this, its impact on AMPK activity would appear to be mediated solely by the binding of AMP to the γ subunit, and as such is understandably the quintessential kinase for energy response activation.

More recently, observations that changes in Ca^{2+} concentrations within the cell can mediate alterations in AMPK activity, lead to the discovery that CAMK kinases (CaMKKs) also play a regulatory role in AMPK activation (57). Calcium is well known as a secondary messenger in many cell systems. The role of Ca^{2+} in the generation of mechanical force in muscle cells is crucial as it binds troponin C, and mediates its migration along actin fibres. CaMKK has sequence and structural homology to the yeast Snf1 kinases Elm1, Pak1 and Tos3, as well as LKB1 (59). It exists in two isoforms - α and β - which are 70% homologous. In skeletal muscle, α is unequivocally

expressed (64, 143); the presence of the β isoform, however, is slightly more controversial, with conflicting observations in the literature (64, 72). Regardless of CaMKK isoform, as calcium levels increase within the cell, calmodulin will rapidly bind available ions. The Ca^{2+}/calmodulin complex can then bind CaMKK enhancing its kinase activity by releasing autoinhibition. The α isoform requires Ca^{2+}/Calmodulin binding for activity, whereas the β isoform exhibits some Ca^{2+} independent activity (130). While LKB1 is accepted as the main AMPK activator, more research is required to elucidate the unique contribution of CaMKK to AMPK activation.

Within the past five years much attention has been directed at TGFβ activated kinase 1 (Tak1) as a possible AMPK activator. Its potential was revealed as Tak1 could rescue the triple Elm1, Pak1, Tos3 knockout in yeast (87). It responds to transforming growth factor β (TGFβ) to activate its kinase activity. Tak1 also exists as complex with the Tak1 associate binding proteins 1, 2, and 3 (TAB1, 2, and 3) (16, 27, 118). *In vitro,* they can form a heterotrimer of Tak1, TAB1 and one of either TAB2 or TAB3; however, only TAB1 is required for activation of Tak1 (71, 96, 111). There are currently no reports on the detection of TAB2 and 3 in skeletal muscle. Tak1 itself contains two important domains, the catalytic kinase domain at the N-terminus and the C-terminal association domain that interacts with TAB2 and TAB3 (16, 27, 118). Activation is achieved through the binding of TAB1 to the catalytic domain which promotes autophosphorylation (71, 96). This association can occur in response to TGFβ, tumour necrosis factor α (TNFα), AICAR and metformin (two chemical activators that will be described in the next section) (121, 149). While its unique role in AMPK activation is still being explored, studies in the heart have revealed an interesting function for Tak 1.

It is clear that Tak1 and LKB1 are both highly expressed in the heart, where AMPK function is vital for the regulation of energy metabolism. The cardio-specific conditional knockout of Tak1 in mice resulted in a WPW like phenotype, similar to what is found within human AMPK γ2 mutations (149). *In vivo,* there was decreased AMPK activity and phosphorylation in the hearts of knockout mice. In cultured cardiomyocytes, the lack of Tak1 blocked oligomycin- (an inhibitor of ATP synthase) and metformin- (a well known activator of AMPK) induced AMPK phosphorylation; it also, seemingly, blocked LKB1 activation (149).

These three AMPKKs can each act in their own unique way to stimulate AMPK activity. Further studies are required to determine their specific contribution to activation within the various cell types, and perhaps to discover other relevant kinases. To counter the activating effects of these kinases, two phosphatases are known to deactivate AMPK in times of sufficient energy. Protein phosphatase 2A (PP2A) and PP2C both work to remove the phosphate group on Thr-172 (35, 128). Their activities are mediated by free AMP, as AMP bound to the AMPK γ subunit prevents dephosphorylation.

Pharmacological and Hormonal Activation

AMPK clearly responds to endogenous stimuli and inhibitors to maintain cellular energy levels. As described above, this occurs through AMP binding, or indirectly, through activation of upstream kinases. At the whole body level, AMPK can also be regulated to control total body energy stores. Indeed, AMPK is highly expressed in the neurons within the hypothalamic region of the brain, a major site of control of

hunger and satiety. In the hypothalamus, addition of leptin, an anorexigenic hormone released from adipose tissues, decreased AMPK activity and eating (8, 84). Conversely, ghrelin, an orexigenic hormone released from the stomach, stimulated AMPK and eating (8, 84). Compellingly, the administration of AICAR, or the adenoviral expression of constitutively active AMPK in the paraventricular nucleus increased food intake (8, 84).

There are a variety of small molecules available that can be used to directly, or indirectly, stimulate AMPK within the cell. The most widely used exogenous activator is AICAR. Transported into the cell through the adenosine transporter, it is rapidly converted to 5-aminoimidazole-4-carboxamide-1-D-ribofuranosyl-5'-monophosphate (ZMP), a structural mimetic to AMP (30, 108, 110). ZMP is reactively inert, but its shape allows it to bind AMPK in the AMP binding pocket stimulating AMPK activity (43, 109). It works without altering the AMP:ATP ratio within the cell, which is highly desirable. However, as it does mimic AMP's structure, it can also act on any other proteins that bind AMP making its actions less specific. For this reason, caution should be used in studies that use AICAR as an AMPK activator. Cool and colleagues performed an extensive screen of small molecules to find more specific AMPK activators (29). One molecule, A-769662, was particularly interesting as it was found to specifically bind and activate AMPK (29). It is a non-nucleoside pyrididone that acts allosterically. The exact mechanism of action is unknown as it binds a heretofore unknown ligand binding site. It binds neither the active site, nor the γ subunit, and does not alter the AMP:ATP ratio (48). However, its action is AMPK-specific and potent with an IC_{50} of 0.7μM as opposed to that of AMP (112uM) (29).

Other small molecules act indirectly by altering cellular concentrations of AMPK activators. Dinitrophenol (DNP) and rotenone both work to modulate AMPK activity by impairing the electron transport chain, disrupting ATP production (42, 58). Rotenone directly binds complex I, inhibiting the oxidation of NADH and impairing the development of the proton gradient required for ATP synthesis. DNP is a lipophilic ionophore that rapidly upsets the proton gradient created across the mitochondrial inner membrane. With the proton gradient across the mitochondrial inner membrane greatly decreased, ATP synthase is unable to produce ATP. Thus, both molecules increase the AMP:ATP ratio to activate AMPK.

Metformin, the most widely prescribed oral antidiabetic agent for treatment of type 2 diabetes mellitus (T2DM), also works to activate AMPK (152). As an antidiabetic agent, it mainly acts through inhibition of gluconeogensis within the liver and improvement of insulin sensitivity in peripheral tissues. Its mechanism of action on AMPK is not entirely understood, but growing evidence suggests that it works in a similar manner to rotenone, inhibiting complex I of the electron transport chain, increasing the AMP:ATP ratio within the cell (36, 97). However, it has been shown that Tak1 presence is required for its effect within the heart (149).

Another class of T2DM medications, the thiazolidinediones (TZDs), also work by activating AMPK within the cell. For example, rosiglitazone and pioglitazone increase AMPK activity, but the mechanisms are, as yet, poorly understood (40). Two studies suggest that they increase the AMP:ATP ratio (40, 74), whereas another study reports no change (76).

There also exists at least one inhibitor, 'Compound C'. This compound is membrane permeable, and when administered to cells (*e.g.,* H-2K skeletal muscle cells, and primary hepatocytes), it results in a reversible drop in AMPK activity (41, 152). Compound C has been shown to compete with ATP for binding to strongly inhibit AICAR's effect of AMPK, but not that of DNP (41, 152). Further investigation showed that Compound C inhibits the adenosine transporter, blocking the entry of AICAR into the cell (41).

Targets of AMPK

The first identified substrate of AMPK was ACC, an enzyme involved in lipid oxidation within the cell (150). ACC catalyzes the conversion of acetyl-CoA to malonyl-CoA which in turn inhibits carnitine palmitoyl transferase 1 (CPT1), a transporter that shuttles fatty acids into the mitochondria for β-oxidation. AMPK activation directly phosphorylates and inhibits ACC; this, in turn suppresses CPT1 inhibition, and increases β-oxidation (Figure 3) (17, 89, 99). ACC exists in 2 forms, ACC1 and ACC2, which vary in not only in their tissue distribution, but also in their cellular localization. ACC1 is ubiquitously expressed, and is the only isoform in white adipose tissue (17, 89). ACC2 is expressed in liver, brown adipose tissue, brain, and is the only isoform in skeletal muscle and heart tissue (2, 62). ACC1 is distributed evenly throughout the cytoplasm, its knockdown results in decreased lipogenesis, signifying its specific cellular role (115). ACC2, alternatively, is anchored to mitochondria, bringing it in close proximity to CPT1, suggesting that it controls the local malonyl-CoA pool responsible for CPT1 inhibition (1). This concept was confirmed in studies of ACC2-

Figure 3. Role of AMPK in Lipid Metabolism. Active AMPK directly phosphorylates and inhibits acetyl-CoA carboxylase (ACC) thereby increasing fatty acid oxidation through a decrease in malonyl-CoA which normally inhibits carnitine palmitoyl transferase 1 (CPT1). AMPK also indirectly increases fatty acid translocase/cluster of differentiation 36 (FAT/CD36) expression to increase fatty acid uptake.

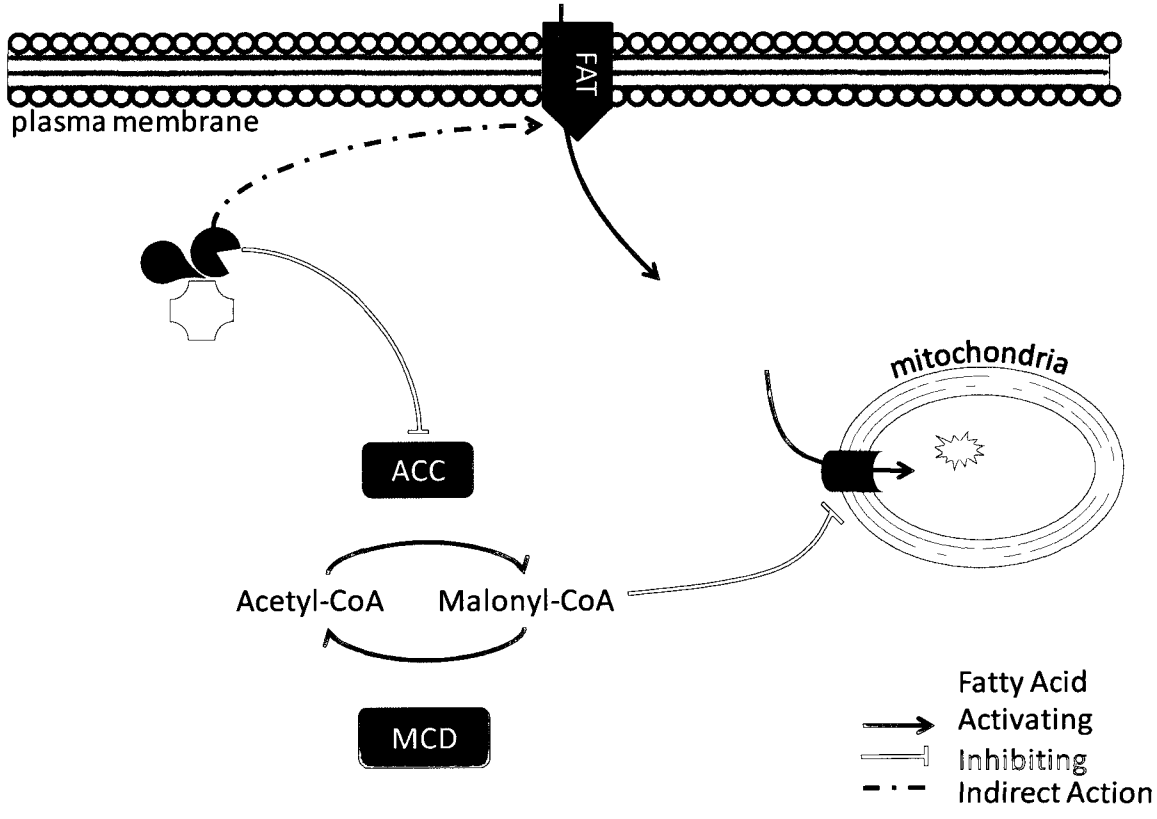
FAT
plasma membrane
mitochondria
ACC
Acetyl-CoA
Malonyl-CoA
MCD
Fatty Acid
Activating
Inhibiting
Indirect Action

specific knockout mice, which demonstrated increased fatty acid oxidation within skeletal muscle, and an overall lean phenotype (3, 4).

ACC is not the only target of AMPK that is involved in lipid metabolism. By altering gene transcription, AMPK works to upregulate other key enzymes involved in lipid metabolism. The first step in cellular lipid metabolism is the uptake of fatty acids into the cell. Fatty acid translocase/cluster of differentiation 36 (FAT/CD36) is a well regulated lipid transporter in the plasma membrane (19). Its expression is regulated by peroxisome proliferator activated receptors (PPARs); in turn, expression and activity of PPARs are regulated by AMPK (75, 104). Upon energy depletion, AMPK acts to upregulate expression of FAT/CD36 and thereby increase fatty acid entry into the cell, while kickstarting the process of ATP production from fatty acid β-oxidation (Figure 3). AMPK also works on the transcriptional activator sterol response element binding protein-1c (SREBP1c) to decrease expression of fatty acid synthesis proteins (39).

Carbohydrates, such as glucose, are generally the preferred fuel source for cells; if they are available, cells will, generally speaking, oxidize them over fatty acids. During times of exertion the first substrate utilized is glucose, either delivered from the blood, or through the breakdown of stored glycogen. AMPK is a key regulator of cellular glucose uptake and glycogen metabolism. Glucose uptake is increased in response to feeding through the action of insulin on the phosphoinositide 3-kinase (PI3K) pathway leading to the phosphorylation of Akt and the increased transport of glucose transporter 4 (GLUT4)-containing vesicles to the plasma membrane (114). AMPK acts through an alternative pathway to shuttle GLUT4 to the membrane and increase

glucose uptake in response to increased cellular fuel demands (45). GLUT4 is sequestered away from the plasma membrane in endosomes that can be rapidly transported to the membrane in response to signals that work to promote glucose uptake (Figure 4). Originally identified as AS160, further research suggested TBC1D1 is actually the target of AMPK's action on GLUT4 cycling (129). During times of low energy storage, AMPK phosphorylates TBC1D1 which promotes its association with the 14-3-3 scaffolding protein (129). This association, in turn, promotes GLUT4 vesicle cycling to the plasma membrane. AMPK also increases expression of GLUT4 through control of gene expression, which will be discussed shortly.

During times of cellular stress, preference will be given for fuel breakdown, as opposed to storage, so that fuels are available to counter the stressors. Glycogen is the major source of stored glucose in the cell. It is maintained in a dynamic process through the action of glycogen synthase (GS) and glycogen phosphorylase (GP). GS works to attach glucose-1-phosphate (G1P) to a nascent glycogen strand, while GP counteracts this action by removing G1P for breakdown through glycolysis. The two counteract each other allowing glycogen to be rapidly synthesized or degraded as the cellular demands change. AMPK can directly phosphorylate and inhibit GS, inhibiting glycogen synthesis, allowing for GP to degrade glycogen (23). An addendum needs to be added to this model though. While AMPK will acutely inhibit glycogen synthesis and deplete glycogen stores in response to activation, it will concomitantly promote glucose uptake (9). Glucose transported into the cell is rapidly converted to glucose-6-phosphate (G6P) through the action of hexokinase. A gross accumulation of G6P can allosterically activate GS, to such an extent that it overrides the phosphate's inhibition

Figure 4. Role of AMPK in Glucose Metabolism. Phosphorylation of Akt substrate 160 (AS160) by AMPK increases association with protein scaffold 14-3-3 which increases glucose transporter 4 (GLUT4) shuttling to the plasma membrane, increasing glucose uptake. AMPK phosphorylates and directly inhibits glycogen synthase (GS) to decrease glycogen synthesis. Under conditions of high glucose uptake, accumulated glucose-6-phosphate (G6P) can lead to a suppression of GS inhibition, and an increase in glycogen synthesis.

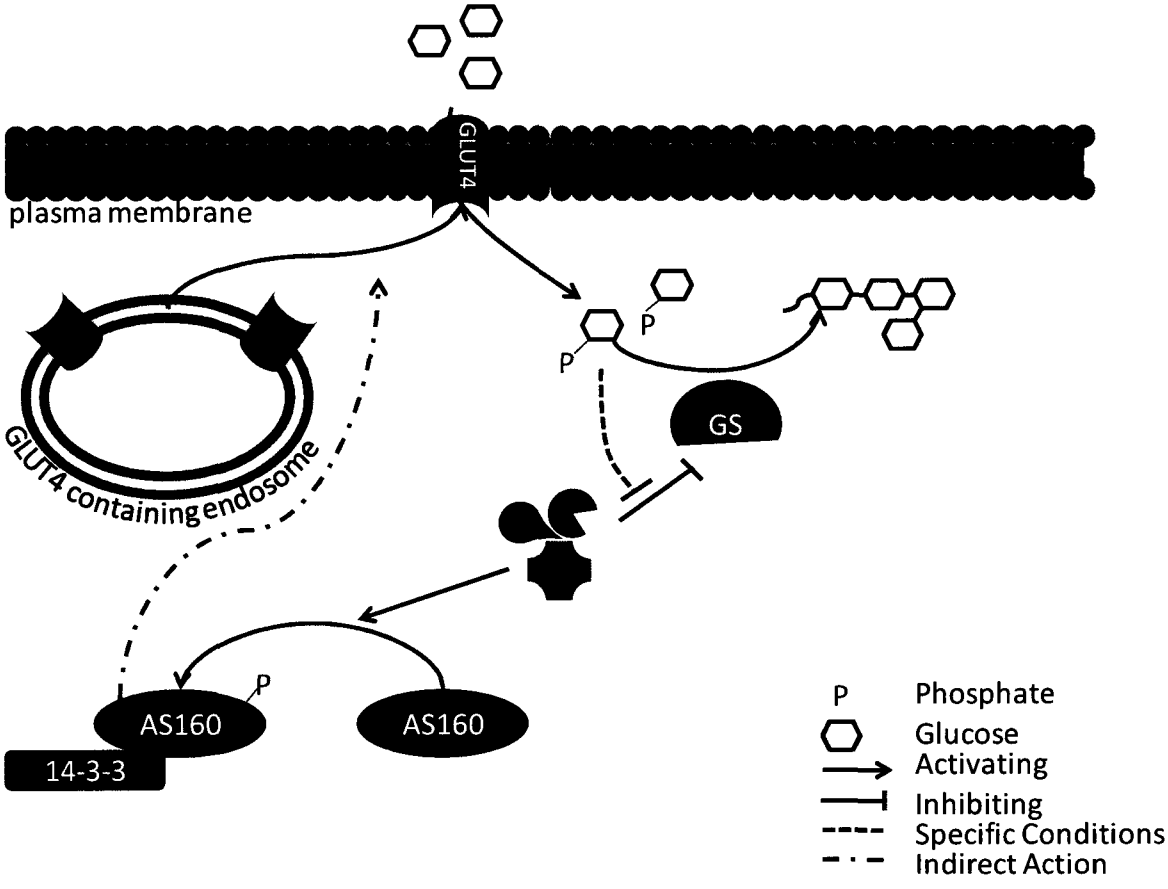
GLUT4
plasma membrane
GLUT4 containing endosome
P
P
GS
AS160
P
AS160
14-3-3
P Phosphate
Glucose
Activating
Inhibiting
Specific Conditions
Indirect Action

(Figure 4) (9). Therefore, an acute or moderate activation of AMPK depletes glycogen through its action on GS, but a chronic activation can lead to accelerated glycogen storage by the increased levels of G6P within the cell.

Glycolysis and β-oxidation create ATP through substrate level phosphorylation and oxidative phosphorylation. AMPK activation also has been shown to increase cellular mitochondrial content. Mitochondriogenesis increases with chronic AICAR administration (142), an effect that is eliminated in mice with impaired AMPK signalling (67, 68). PPARγ coactivator-1α (PGC-1α) is a transcriptional co-activator that controls expression of several mitochondrial genes, as well as itself and GLUT4. It can also be directly phosphorylated by AMPK to promote its association with PPARγ and subsequent transcription of target genes (75). Nuclear respiratory factor 1 and 2 (NRF1 and 2) can homodimerize as well as interact with PGC-1α to act as transcription factors that target genes encoding mitochondrial DNA and controlling mitochondriogenesis (133, 134). Expression of NRF 1 and 2 dramatically increases in response to AMPK activation from ATP depletion (15). Activation of AMPK, therefore, can increase mitochondrial content, as well as the complexes required in the electron transport chain for increased ATP synthesis.

As well as enhancing ATP production, AMPK inhibits non-essential ATP demanding processes. Protein synthesis is an energetically expensive task, and is halted to variable extents in times of energy depletion (106). AMPK activates the mammalian target of rapamycin complex (mTORC) pathway to inhibit protein synthesis (70, 105). mTORC is considered to be a major regulator of protein translation, cell growth and apoptosis within mammalian cells. Upstream, mTORC is

activated by the GTPase Rheb which is in turn inhibited by the GTPase activated protein (GAP) tuberous sclerosis protein 1/2 (TSC1/2). During feeding, insulin stimulation leads to inhibition of TSC1/2 by p-Akt phosphorylation of Ser-533 ultimately relieving inhibition and promoting protein synthesis (50). During stress, however, TSC1/2 is phosphorylated by AMPK at Ser-398, activating it, stimulating its repression of the mTORC pathway and blunting protein synthesis, promoting ATP conservation (Figure 5) (18, 140).

AMPK in Health and Disease

As such a potent regulator of cellular and whole body metabolism, it is reasonable to expect that AMPK would play a role in several metabolic diseases. Obesity is rapidly becoming one of the most prevalent metabolic diseases worldwide. According to the World Health Organization (WHO) about 400 million people globally are afflicted with obesity, and that number is expected to increase almost 6 times by 2015 (139). Obese individuals are defined by having a BMI greater than 30 kg/m^2. In several rodent models of obesity AMPK signalling is impaired in various tissues including the heart, skeletal muscle and liver (13, 78, 122, 126, 135). However, diet-induced obesity in other mouse strains, have negligible differences in AMPK signalling, consistent with the fact that the mechanisms underlying obesity and related diseases are complex (80, 136). Genetic screens of obese populations have revealed some association with AMPK signalling, but fairly negligible amounts (11, 127).

T2DM is strongly associated with obesity and is initially characterized by a development of insulin resistance (*e.g.*, in the liver and periphery), and eventually by the loss of pancreatic β cell insulin production. As AMPK can modulate glucose uptake

Figure 5. Control of Protein Synthesis by AMPK. Active mammalian target of rapamycin complex (mTORC) promotes cell growth and protein synthesis. It is activated by the Rheb GTPase which is, in turn, inhibited by tuberous sclerosis protein 1/2(TSC1/2). Insulin stimulation leads to TSC1/2 inhibition by Akt phosphorylation, thereby activating mTORC and increasing protein synthesis. Active AMPK, from increased AMP:ATP for example, phosphorylates and activates TSC1/2 ultimately inhibiting protein synthesis.

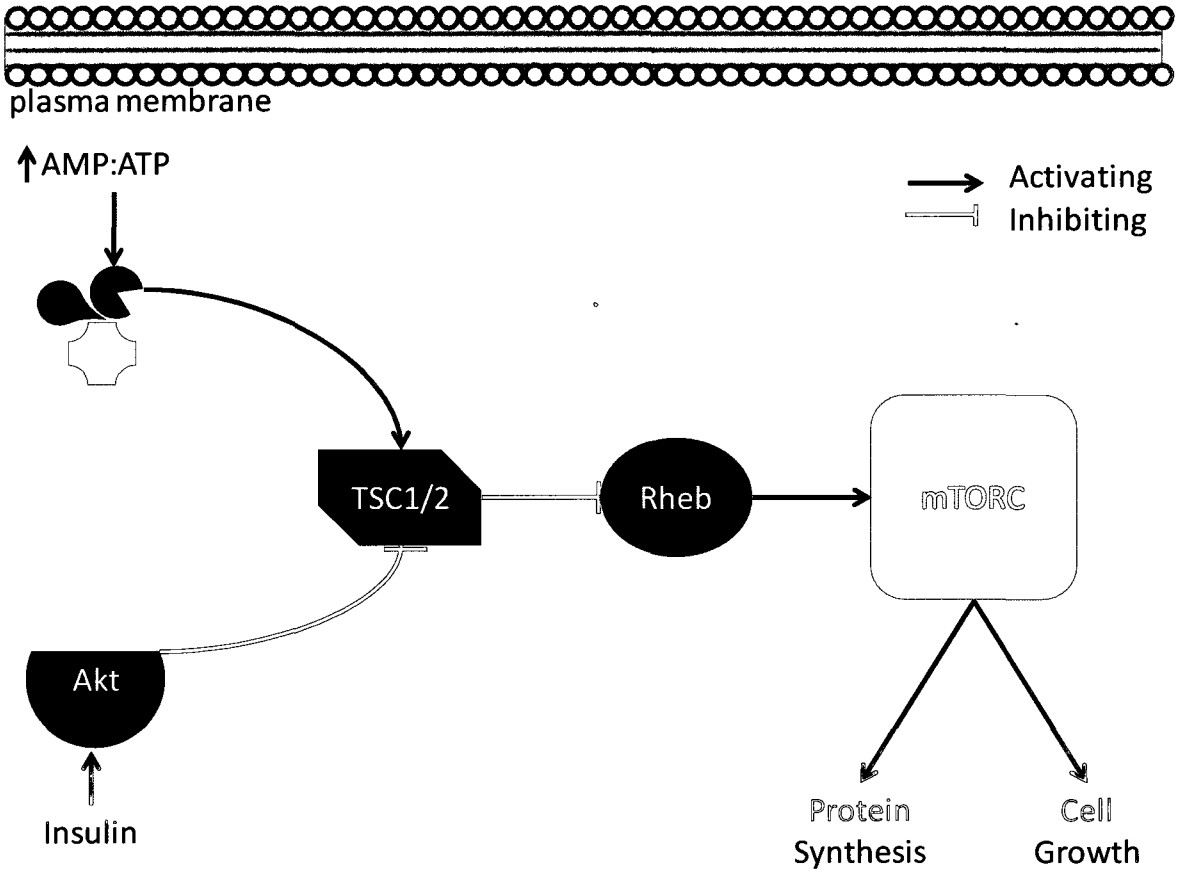
plasma membrane
AMP:ATP
Activating
Inhibiting
TSC1/2
Rheb
mTORC
Akt
Insulin
Protein
Synthesis
Cell
Growth

through GLUT4 independent of the insulin receptor, it is an attractive therapeutic target. As discussed above, metformin has long been used to treat T2DM, and it is now thought to function primarily through the inhibition of mitochondrial Complex I (97). Though, more research is needed for a better understanding of the mechanisms of metformin action (*e.g.,* altered mitochondrial production of reactive oxygen species at Complex I).

The impact of AMPK on metabolic health and disease has been advanced by studies of naturally occurring mutations in AMPK genes. Mutations are generally fairly rare, but can have strong impacts on metabolism and cellular fuel storage. The first mutation to be discovered was in Rendement Napole (RN^-) pigs (52, 83). An observation that certain pigs within a group produced sour tasting meat, resulted in the discovery that these pigs exhibited increased glycogen storage within their skeletal muscle in relation to a mutation in the γ3 subunit – R225Q (95). The mutation led to an increase in basal AMPK activity. As described above, while AMPK can inhibit glycogen synthesis, prolonged activation leads to increased cellular levels of G6P through the action of AMPK on GLUT4; this counteracts the normal inhibition of GS by AMPK, leading to stimulated glycogen synthesis. In humans a homologous mutation was found in an Ottawa population. The R225W mutation on the human γ3 subunit resulted in increased glycogen storage and decreased triglyceride storage in skeletal muscle as well as increased glucose uptake in exercised muscle and a resistance to fatigue (31, 32). Much like the R225Q mutation found in pigs, the R225W mutation increased basal activity in the AMPK complex (31). The increased skeletal muscle glycogen storage has a generally beneficial effect overall, apparently conferring affected

individuals the ability to excel at endurance sports. Within the heart, however, increased glycogen storage can cause severe impairments to function.

Located within the same region as the γ3 mutations described, the γ2 R302Q mutation also results in amplified glycogen storage, specifically in the heart (38, 47). The accumulated glycogen granules interfere with electrical conductance, leading to the development of a less efficient accessory pathway, which can be identified on an electrocardiogram (ECG) by a pre-excitation and delta wave (46). The heart thus becomes enlarged and requires the administration of external shocks through an implanted pacemaker. Originally there was great controversy over the exact impact of the R302Q mutation on AMPK activity (5, 12, 21, 38, 46, 51, 119). The increased glycogen storage suggested a loss of function mutation which is incapable of appropriately inhibiting GS. More recently the consensus has shifted towards the recognition that its impact is as a gain of function mutation, impairing glycogen inhibition through accelerated glucose uptake (91). The altered residue is located in an identical location to the well studied γ3 mutations – within the AMP/ATP-sensing CBS1 domain (46). It can been speculated that residue shift from a positively charged amino acid, to a bulky hydrophobic residue can alter AMP or ATP binding, resulting in changes in sensitivity to and activation by increases in the AMP:ATP ratio.

As discussed above, the γ2 subunit is the predominant γ subunit expressed in the heart, explaining why its impact is so severe. The γ2 isoform mRNA is expressed in skeletal muscle as well, though protein detection is difficult as the antibodies developed for immunoblotting are non-specific and only weakly associated with γ2. Families of patients within the Ottawa region express this rare mutation and are

afflicted with WPW syndrome (47). Under the supervision of Dr. Michael Gollob of the University of Ottawa Heart Institute, these patients are monitored and their condition is studied in a clinical setting. Regardless of their potential for limited activity due to strain on their heart, they are generally extremely active and there is no history of obesity or diabetes. This could be due to an impact of the γ2 subunit on skeletal muscle metabolism, similar to the γ3 mutations, but to a more moderate extent. As muscle biopsies of heart tissue are invasive and potentially more dangerous, skeletal muscle biopsies were chosen as a method to examine the R302Q mutation within human primary muscle tissue. By collecting skeletal muscle biopsies from affected subjects and closely matched controls, we hope to elucidate the potential contribution of the γ2 R302Q mutation on overall skeletal muscle metabolism, and gain insight into the overall mechanism of action of this mutation.

Objectives

1) To investigate the effect of the AMPK γ2 R302Q mutation on human skeletal muscle metabolism and directly measure its impact on AMPK activity.
2) To exogenously express the human γ2 mutation in a skeletal muscle cell line to further probe the metabolic implications of this mutation.

Hypothesis

We hypothesize that the γ2 R302Q mutation results in increased basal AMPK activity. Further we predict increased basal activity, decreased triglyceride content as well as increased glycogen content within both the affected human tissue preparations and in the infected C2C12 myotubes expressing the γ2 protein.

Methods

Human Skeletal Muscle

Muscle Biopsies

A total of 13 biopsy samples were taken from consenting subjects, four of which were patients carrying the R302Q variant. Subjects fasted for 12h and were asked to abstain from physical exertion 48h prior to the procedure. Using a 5mm Bergstrom needle, percutaneous skeletal muscle biopsies of the *vastus lateralis* were taken under local anaesthesia with 1% lidocaine. 70-90mg of muscle was obtained. 30mg was flash frozen in liquid nitrogen for RNA extraction and gene expression, the latter of which will be processed and analyzed in the future by our research group, 15-20mg was frozen in O.C.T. (optimal cutting temperature) compound for histology, the methods are described in a separate section below.

Ex vivo Histology

Immediately after the biopsy, a suitable sized piece of muscle (approximate 15-20mg) underwent 20 minute incubations through each step of a sucrose gradient ranging from 5% sucrose in phosphate buffered saline (PBS) to a final 20% w/v sucrose. To obtain an appropriate temperature for freezing, isopentane was frozen using liquid nitrogen then thawed until the isopentane formed a slurry of liquid and frozen material. A histology cassette containing the muscle of interest surrounded by O.C.T. compound was quickly submerged into the slurry and held for up to 10 seconds before being transferred, in a sealed plastic bag, to -80°C for storage.

Frozen tissue embedded in O.C.T. compound was later cut into 10μm cross-sections using a Microm cryostat (Thermo Scientific; Two Rivers, WI) and mounted on Superfrost slides. Staining was undertaken to determine fiber type ratio, glycogen content, and intramyocellular lipid content (IMCL). Types 1, 2a, and 2x fibers were indentified using A4.480, N2.261 and BFF3 as primary antibodies, respectively (Developmental Studies Hybridoma Bank). Specific fiber types were stained red (Type 1), blue (Type 2a), or brown-black (Type 2x) using SK-5100, SK-5300, and SK-5200, respectively (Vector Labs).

Preliminary glycogen determinations were undertaken using periodic acid Schiff (PAS) staining, resulting in a purple stain whose intensity is proportional to the stored glycogen within the cell. Oil Red O was used to determine IMCL content, by staining lipid deposits. All slide images were analyzed using ImageJ (freeware obtained from http://rsbweb. nih. gov/ij/).

Satellite Cell Isolation

The remaining 25-30mg was used for satellite cell isolation and cell culture. The tissue was minced then digested using a 0.25% trypsin-EDTA solution (TE) in a specialized digestion flask with indented sides at 37°C with a stir bar to allow for constant turbulence. The liberated cells and remaining tissue fragments were plated on 6cm cell culture plates and grown to approximately 60-70% confluency in 3 mL growth medium (GM: Ham's F10 medium supplemented with 2% antibiotic-antimycotic, 2. 5ug/μL gentamycin, 15% fetal bovine serum, 0. 5mg/mL bovine serum albumin, 1μM dexamethazone, 10ng/mL epidermal growth factor, 0. 5mg/mL fetuin, and 25pmol insulin).

Satellite cells were isolated from the remaining cell population (*e.g.*, fibroblasts) using MACS magnetic sorting for CD56 using primary anti-5.1H11 antibody (Miltenyi Biotec; Bergisch Gladbach, Germany). Magnetically labelled cells were isolated, eluted, and maintained in GM as previously described (31). Cells were lifted from four separate 6cm dishes by incubation with 1mL of TE for 3 min at 37°C. One volume of growth media was added to stop the proteolysis reaction. The cell suspension was transferred to a 15mL Falcon tube, as the plates were washed with 1 mL GM to collect any remaining cells. Cells were spun for 7 min at 700g at room temperature, the supernatant was eluted and the cell pellet was gently resuspended in 200µL CD56 buffer (100µL bovine serum albumin (BSA) (250mg/mL), 0. 5mL EDTA (200mM), 125 µL glucose (2M) brought to a final volume of 50mL with PBS-AG), then 40µL of anti-5. 1H11 microbead-conjugated antibody (diluted 1:1 in glycerol) and was incubated at 4°C for 20 minutes in the dark, halfway through the incubation period, the samples were gently agitated to ensure optimal suspension of the cells. Cells were washed with the addition of 1mL of CD56 buffer at 4°C then centrifuged at 700g for 7 min at room temperature. During this time, the magnetic column was set up in the hood, and dishes were prepared with GM for the purified cell samples.

The cell pellet was resuspended in 500µL CD56 buffer at 25°C, while the magnetic column was washed with 500µL PBS-AG (137mM NaCl, 2. 7mM KCl, 8mM Na_2HPO_4, 1. 5mM KH_2PO_4 supplemented with 2% antibiotic-antimycotic and 2. 5ug/µL of gentamycin). Following manufacturer's directions, the labelled satellite cells were separated from the unlabelled remaining cells. All 1mL of the labeled cell suspension was plated onto one small flask, while 500µL of the unlabeled cell suspension was

plated onto another small flask and later stored in liquid nitrogen. At a future date the unlabelled cells can be regrown to potentially harvest more satellite cells if needed.

Cell Maintenance

Cells were grown in small 25cm^2 flasks until 60-80% confluency was achieved, then split and maintained in larger 75cm^2 flasks. At 70-80% confluency, cells were differentiated into myotubes by changing to differentiation media (DM: Low Glucose Dulbecco's modified Eagle medium (DMEM) supplemented with 2% heat-inactivated horse serum, 2% antibiotic-antimycotic, and 2. 5ug/mL gentamycin).

Glycogen Content of Cultured Cells

Cells were differentiated for 7 days to allow for maximal differentiation of myoblasts into myotubes. Cells were lifted using TE, then centrifuged at 700g. The cell pellet was resuspended in 200μL glycogen assay buffer (20mM KH_2PO_4, 10μM $CaCl_2$, 1mM $MgCl_2$, pH 6. 1) then lysed by 5 freeze-thaw cycles in liquid nitrogen and a 37°C water bath, with care taken to not allow the samples to warm beyond 4°C. The freeze-thaw process was optimized to compare differences between freeze-thaw, freeze-thaw with storage at -80°C, and direct addition of lysate to ammonium sulfate and potassium hydroxide digestion buffer, with no significant differences in measured glycogen content observed. As such, freeze-thaw with storage at -80°C was utilized as it afforded the ability to measure multiple samples across a single experiment day. 50μL of the cell solution was subsequently digested in 500μL saturated ammonium sulfate in 30% potassium hydroxide in a boiling water bath for 20min, the remaining 150μL was retained for protein content analysis using the BCA protein assay. Glycogen was

subsequently precipitated out of solution with the addition of 600μL ice-cold 95% ethanol then isolated by spinning at 4000g for 15min at 4°C, and finally resuspended in 500μL ddH_2O.

Glycogen content was determined with the addition of a colorimetric indicator (0. 2% anthrone in 98% sulfuric acid) and incubation in a boiling water bath for 20 min. 1mL of the anthrone indicator was added slowly and carefully. Much care was taken as the temperature of the sample increased with the addition of the high volume of sulfuric acid. A glycogen standard curve using isolated oyster glycogen (Sigma) quantified the amount of glycogen present in our samples by comparing absorbance values at 620nm. Results were then standardized to the cellular protein content using a BCA assay.

Cellular Triglyceride (TG) Storage

On the sixth day of cellular differentiation the medium above the cells was changed to differentiation medium containing 2% BSA, 200nM oleate; control cells were changed to 2% BSA DM lacking oleate. 18h later the differentiated cells were lifted using TE, and spun at 700g for 7min at room temperature. The supernatant was aspirated and the cell pellet was resuspended in 1.1mL TG buffer (25mM Tris-HCl, 1mM EDTA pH 7. 5), and stored at -80°C until experiment day.

On the day of analysis 1mL of the sample was transferred to a stoppered glass test tube, while the remaining sample was retained for a Bradford protein assay. 3.75mL of a 2:1 (v:v) methanol to chloroform mixture was added to the sample then mixed for 10 min using a benchtop vortex mixer. An additional 1mL of chloroform was

added to the solution and then mixed an additional 1 min. Finally 1mL of ddH_2O was added and the solution was mixed for 1min before being spun at 3000g for 10 min.

Using a glass pipette the lower, organic, phase was transferred into a new 12x75mm glass test tube, with care taken not to disturb the interphase or upper aqueous phase. Using a special N_2 (g) apparatus, the solvent was evaporated to dryness under a constant stream of N_2 at 45°C for approximately 10 min. The lipids remaining in the test tube were immediately dissolved in either 60µL (for untreated) or 100µL (for fatty acid treated) of isopropanol using a vortex, to ensure the TG values were measurable by a standard curve.

TG content was analyzed using the L-Type TG M assay kit (Wako Diagnostics; Richmond, Virginia). A standard curve was constructed using the Wako Multi-Lipid Calibrator set, as per manufacturer's instructions. 15µL of each 'unknown' sample was loaded in triplicate onto a 96 well plate, along with the 15µL aliquots for the standard curve. Then 90µL of the kit's Reagent 1 was added to all wells with care to avoid the formation of bubbles and the contents of the plate were mixed by gentle agitation. The plate was then sealed with a plastic plate sealer to minimize oxidation of lipids and incubated at 37°C for 5 min.

Using a Spectramax M2 spectrophotometer (Molecular Devices/MDS; Toronto, ON), the absorbance of each well was measured at 600nm with a reference wavelength set at 700nm. This measurement was used as the sample blank. Next, 30µL of the kit's 'Reagent 2' was added to each well, mixed by gentle rotation, sealed and incubated for 5min at 37°C. Absorbance was read at 600nm with a reference wavelength of 700nm, and the final absorbance was obtained by subtracting the first measurement from the

second. Sample concentrations were determined using the standard curve and the results were standardized to the protein content of samples.

Western Blot Analyses

Cells were differentiated for 7days in DM, lifted with TE then spun down at 700g for 7min. The resultant pellet was resuspended in 350μL radioimmunoprecipitation assay (RIPA) buffer supplemented with 1mM sodium orthovanadate (phosphatase inhibitor) and 1X Roche Protease inhibitor cocktail (Roche; Mississauga, ON). Samples were stored at -20°C until needed. Alternatively, protein samples from the SAMS peptide assay were stored in 5X sample buffer (50mM Tris-HCl, 25% Glycerol, 2% SDS, 14.4mM 2-mercaptoethanol, 0.2% bromophenol blue) for later analysis.

The concentration of the sample was determined using a BCA protein assay. 5X sample buffer was added then the new concentration was calculated for the resultant volume. Depending on the specific protein being probed 10-30μg of protein was loaded into each well of a 7%-12% SDS PAGE gel in a minigel system (BioRad mini; Mississauga, ON). Gels were run approximately 1h at 150V in a running buffer (30mg/mL tris, 142mg/mL glycine, 0.1% SDS). Transfers occurred at room temperature at 120V for 1 hour in a transfer buffer (72mg/mL tris, 15mg/mL glycine, 20% v/v methanol) using a mini-Transblot cell (BioRad). After transfer, membranes were stained (0.1% w/v Ponceau in 5% v/v acetic acid) to determine the approximate efficiency of protein transfer, and then washed in water and TBS-T (10mM Tris-HCl, 100mM NaCl, 0.1% Tween-20, pH 8.0).

Membranes were blocked in 5% w/v skim milk powder in TBS-T for 1 h at room temperature. Primary antibodies were incubated with the membrane in a sealed

plastic bag overnight at 4°C, and were diluted in 5% w/v BSA in TBS-T (p-ACC, ACC, p-AMPK, p-GS, GFP: 1:500; AMPK, GS, Complex III, β-actin: 1:1000). Secondary antibodies were diluted 1:2000 in 5% skim milk powder and incubated 1h at room temperature (anti-rabbit for all primary antibodies except GFP and Complex III which required anti-mouse).

A 1:1 mixture of the enhanced chemiluminescence solutions (Super Signal West Pico Chemiluminescent Substrate, Thermo Scientific; Rockford, IL) was applied to the membranes. The images were developed in a dark room on ECL film (Amersham/GE; Buckinghamshire, UK). Membranes were stored in TBS-T at 4°C for up to a year.

AMPK Activity of Isolated Protein from Cultured Cells

Protein Extraction

Seven day differentiated cells were washed twice with PBS-AG (37°C), then lysed in ice-cold AMPK lysis buffer (30mM Hepes, 2.5mM EGTA, 3mM EDTA, 70mM KCl, 0.1% NP-40. pH 7.4 stored at 4°C and supplemented with 20mM β-glycerophosphate, 20mM NaF, 2mM $NaPP_i$, 1mM Na_3VO_4, 200μM phenylmethylsulfonyl fluoride (PMSF), 1μM pepstatin A on the day of the experiment) with constant agitation for 5 min on ice. Lysate was pooled from 2-4 large flasks then distributed evenly across Eppendorf mini-tubes and centrifuged at 14,000g for 5min at 4°C to pull down large cell fragments. 500μL of the supernatant was divided evenly between ice cold Eppendorf mini-tubes and 1 volume of 30% polyethylene glycol (PEG) was added to gently precipitate the protein. After 60min incubation on ice, the PEG sample was centrifuged at 18,000g for 10min at 4°C. The entire supernatant was aspirated, and the resultant PEG protein

pellet was flash frozen in liquid nitrogen, then stored at -80°C until the day of experiments.

Immunoprecipitation

Immunoprecipitation (IP) beads (Dynabeads; Invitrogen, Burlington, ON) were incubated with 10μg anti-AMPK α1 and 10μg anti-AMPK α2 antibody (generous gift of Dr. Graham Hardie) in "Antibody binding and washing buffer" for a total volume of 200uL; this was mixed for 1h at 4°C. Meanwhile frozen PEG-purified protein sample (typically 6 Eppendorf mini-tubes, representing 2 large flasks of cells) were resuspended in 200μL IP buffer (50mM Tris-HCl, 150mM NaCl, 50mM NaF, 5mM Na pyrophosphate, 1mM EDTA, 1mM EGTA pH 7.4, supplemented with 5mg/mL soybean trypsin inhibitor, 100μM PMSF on the day of the experiment). Protein concentration was determined using a standard BCA assay.

Antibody-conjugated IP beads (Ab-beads) were washed in "Antibody binding and washing buffer" then 100μg of the patient sample was added, and the remainder of the 250μL final was provided by IP buffer (the remaining sample was frozen in sample buffer for later analysis by Western blot). Ab-beads were incubated with the sample for 2h at 4°C with constant oscillation on a rotary mixer. The protein conjugated Ab-beads were washed 3 times with 200μL "Washing buffer" then resuspended in 100μL and transferred to a new 1.5mL tube. The supernatant was then removed and the immunopurified protein and beads were resuspended in 70μL AMPK reaction buffer (50mM Na Hepes pH 7.0 supplemented on the day of experiments with 1mM DTT, and 0.02% Brij-35).

Activity Assay

ACC, a known substrate of AMPK, is phosphorylated at Ser 79. A peptide was developed around the ACC phosphorylation sequence: HMRSAMSGLHLVKRR, also commonly referred to as the 'SAMS' peptide. The SAMS peptide assay is considered to be the "gold standard" for measuring AMPK activity (34, 54, 146); however, due to challenges associated with the assay, the activity of AMPK is more commonly determined using simpler methods, such as ACC phosphorylation.

The protein sample was divided evenly between three reaction tubes for each of the three conditions: background, basal, and AMP-activated. For each condition, master mixes were created, such that they were all one third [P^{32}]-ATP solution (1mM ATP in 25mM $MgCl_2$, with hot ATP diluted to 1μCi/μL). The AMP-activated reaction mix contained one third AMP solution (1mM ATP in ddH_2O), and the basal and activated reactions also contained one third SAMS peptide (1mM in ddH_2O). All of the above were supplemented with AMPK reaction buffer to bring the total volume to 30μL prior to the addition of 20μL of immunopurified AMPK solution. All of the reaction vessels were kept on ice prior to their transfer to a 30°C incubator for 15min to allow the reaction to progress. After this, the samples were again placed on ice to stop the reaction. A 20μL aliquot of the reaction mixture was blotted onto 1cm^2 phosphocellulose squares. After sitting for approximately 1min, the squares were washed twice in 1% phosphoric acid solution (5min each), followed by a quick rinse in water, and then in acetone. The squares were then allowed to dry completely at room temperature. A 1μCi standard was blotted onto two separate unwashed squares to allow for subsequent calculations for the conversion of cpm to μCi and thereby [^{32}P]-

ATP incorporation. The radioactivity was measured in scintillation vials containing 5mL of scintillation fluid (Biodegradable counting scintillant, Amersham/GE; Buckinghamshire, UK) and measured on a 1219 Rack beta scintillation counter (LKB Wallac; Mt Waverley, Australia) at 60 seconds for each vial. Basal and activated values were subtracted from the background counts to determine AMPK specific activity, and eliminate any confounding kinase contamination.

C2C12 Adenoviral Sytem

Adenovirus was used in the C2C12 mouse skeletal muscle cell line to express the human AMPK γ2 protein or the R302Q variant. The virus was purchased from Dr. Jason Dyck's lab (University of Alberta), in a purified and titred form.

C2C12 cells were carefully grown up in C2C12 growth media (C2GM: 25mM glucose DMEM supplemented with 10% FBS, 2% antibiotic-antimycotic and gentamycin) with special care taken to prevent the myoblasts from becoming confluent, then differentiated for 6 days in C2C12 differentiation media (C2DM: 4. 5mM glucose DMEM supplemented with 2% FBS, 2% antibiotic-antimycotic and gentamycin). On the fourth day of differentiation, adenoviral infection was begun. Virus was infected at a multiplicity of infection (MOI) of 100:1 for the WT expressing virus, and 150:1 for the R302Q variant in 1mL of Opti-MEM for 5 h. Optimal MOI was determined previously by incubation with varying MOIs to ensure optimal infection, by fluorescence microscopy detection of expressed viral GFP, and reasonable protein expression by western blot. The cells were then overlaid with the 2mL C2DM for the remainder of differentiation (43 more h). On the seventh day, (*i.e.,* 48 h after infection) cells were harvested for western blots, and glycogen content determinations as

described above. For measurements of triglyceride content, the cells were only overlaid with 1mL of C2DM after infection. 30 h post-infection, the cells were again overlaid with a 2mL C2DM supplemented with 4% BSA and, for the treated cells, 400nM oleate, such that, after addition, the final concentration of BSA and oleate is comparable to the treatment given to the primary human cells (2% BSA with 200nM oleate).

Statistical Analysis

Statistical analyses were carried out using Microsoft Office Excel 2007. Unpaired, unmatched, one tailed t-tests were used with the human samples to compare between the two genotypes, while one-way ANOVAs were used to examine the three different C2C12 groups, unless otherwise indicated.

Results

Human Samples

AMPK γ2 R302Q Patient Population

Affected patients are part of two distinct families within the Ottawa area. *Vastus lateralis* biopsies were collected from our four affected subjects over the course of four years (Table 1). Unfortunately the myocytes from one of those samples (B), are no longer viable. Since our patient sample size was so small, we allotted at least two matched control subjects for each affected subject. While each pair is well matched, overall there is a great deal of variability in the ages of our participants. Of our affected subjects, one was highly physically active (referred to as 'D'), much more so than the other members of the affected group. Her control was well matched for degree of physical activity, but this subject was unique in this regard.

Ex Vivo Histological Analyses

Skeletal muscle is a heterogenous tissue containing myofibers that can be classified as three main types – highly oxidative type 1, and glycolytic types 2a and 2x. All of our biopsy samples were from the mixed fiber muscle group the *vastus lateralis*. Sections of muscle were differentially stained using antibodies specific for each of the three major myosin heavy chains. The results are presented in Figure 6, with each group possessing a fiber type ratio of approximately 50% type 1, 35% type 2a and 14% type 2x. There were no statistically significant differences in the proportions of the three major fiber types between the affected and control subject groups.

Table 1. Patients Recruited to the Study. Matched pairs of subjects indicated by a shared letter. Subjects matched by age, body mass index (BMI) and gender. *indicates samples unable to be grown in culture; ⍰ indicates insufficient sample for histological analysis.

R302Q					Matched Control				
Subject	**Age**	**BMI**	**Gender**	**Biopsy**	**Subject**	**Age**	**BMI**	**Gender**	**Biopsy**
A	59	24.5	M	Jun 20 06	A1	61	27	M	May 29 08
					A2	57	22	M	Mar 18 09
B *[redacted]	27	25.3	M	Jan 31 07	B1	26	24.3	M	Oct 16 08
					B2	27	25	M	Oct 21 08
C	20	22.6	M	Nov 22 07	C1	22	21.9	M	Feb 1 08
					C2	21	21	M	Nov 6 08
					C3	22	22.9	M	Nov 27 08
D	32	21.2	F	Jun 25 09	D1	33	21.6	F	Aug 21 09
					D2 *	32	21.2	F	Sept 29 09

Figure 6. Fiber Type Ratio of *Vastus Lateralis* Samples. A) Representative imaged of stained 10um sectioned stained, left: control; right: R302Q. Type 1 fibers stained red with A4.480; Type 2a fibers stained blue with N2.261; Type 2x fibers stained brown with BFF3. B) Quantification of fiber type proportions. Mean +/- SEM; n:3,10; average fiber count per sample: 407; $p>0.05$ with one-way ANOVA.

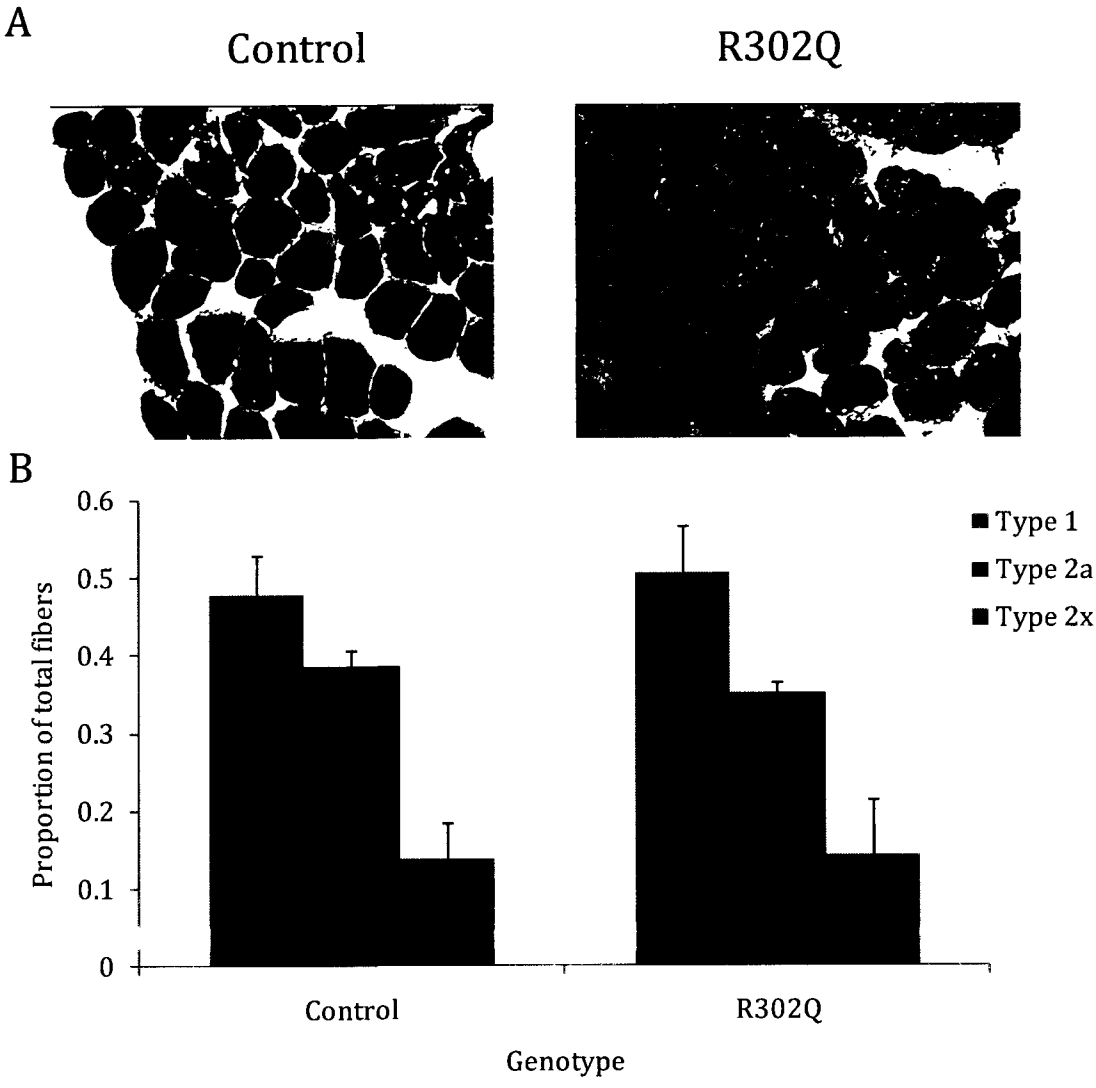
A
Control
R302Q
B
Proportion of total fibers
0.6
0.5
0.4
0.3
0.2
0.1
0
Type 1
Type 2a
Type 2x
Control
R302Q
Genotype

Skeletal muscle glycogen content, assessed by PAS staining of the sectioned *vastus lateralis* was not significantly different between samples from affected subjects and controls. These results are shown in Figure 7. Note, however, that there was a high degree of variability in glycogen staining, particularly in muscle samples from control subjects. Not surprisingly our three highly active individuals (identified in Figure 7 as 'D'), exhibited the highest glycogen pools, though again there appeared to be no difference between samples from the affected subject and her two matched control subjects.

Oil Red O staining of *vastus lateralis* sections was used to measure IMCL as neutral lipid droplets. Samples were available from only two of the affected subjects (C, D), they were compared against their matched controls, as well as against the entire control population. Not surprisingly, the highly active subjects had high muscle lipid content, though, intriguingly, both affected subjects measured had equally high lipid contents as shown in Figure 8. When compared against all control subjects, the affected subjects had significantly greater lipid content in their *ex vivo* samples (unpaired, one-tailed t-test; p=0.0015). Comparison against only their matched control subjects yielded only a trend for increased lipid content (unpaired, one-tailed t-test; p=0.07)

In Vitro Studies of Human Primary Myotubes

Carbohydrate Storage

Direct measurement of glycogen content is a good indicator of the state of carbohydrate storage within the cell. Differentiated human muscle cells were collected

Figure 7. Glycogen Content of *Vastus Lateralis* Samples. A) Fibers stained with Periodic Acid Schiff (PAS), glycogen content relative to stain intensity (Left: Control; Right: R302Q). B) Quantification of stain intensity as measured by integrated density. Scatter points indicate individual measurements grouped by affected patient. Mean +/- SEM; n: 9,3; $p>0.05$.

A

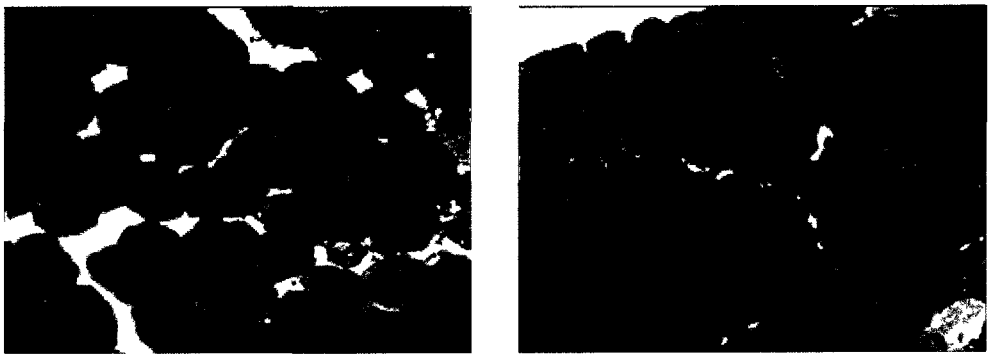
Control
R302Q

B

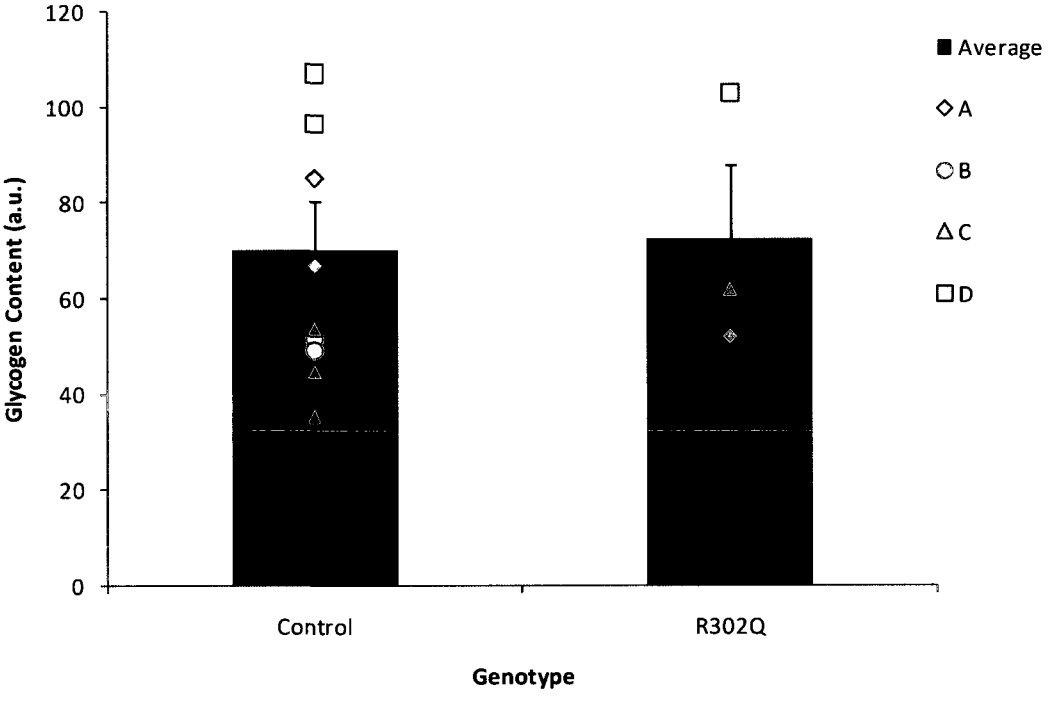
120
100
80
60
40
20
0
Glycogen Content (a.u.)
Average
A
B
C
D
Control
R302Q
Genotype

Figure 8. Lipid Content of *Vastus Lateralis* Samples. A) Oil Red O staining of lipid droplets in human muscle fibers (Left: control; Right: R302Q). B) Quantification of lipid content by determinations of stain intensity as measured by integrated density. Bars represent average of affected subjects and only their specific matched control subjects. Scatter points represent individual patient measurements. Matched Control and Affected Subjects: mean +/- SEM; n: 5,2; p: 0.07 for one tailed, unpaired t-test..

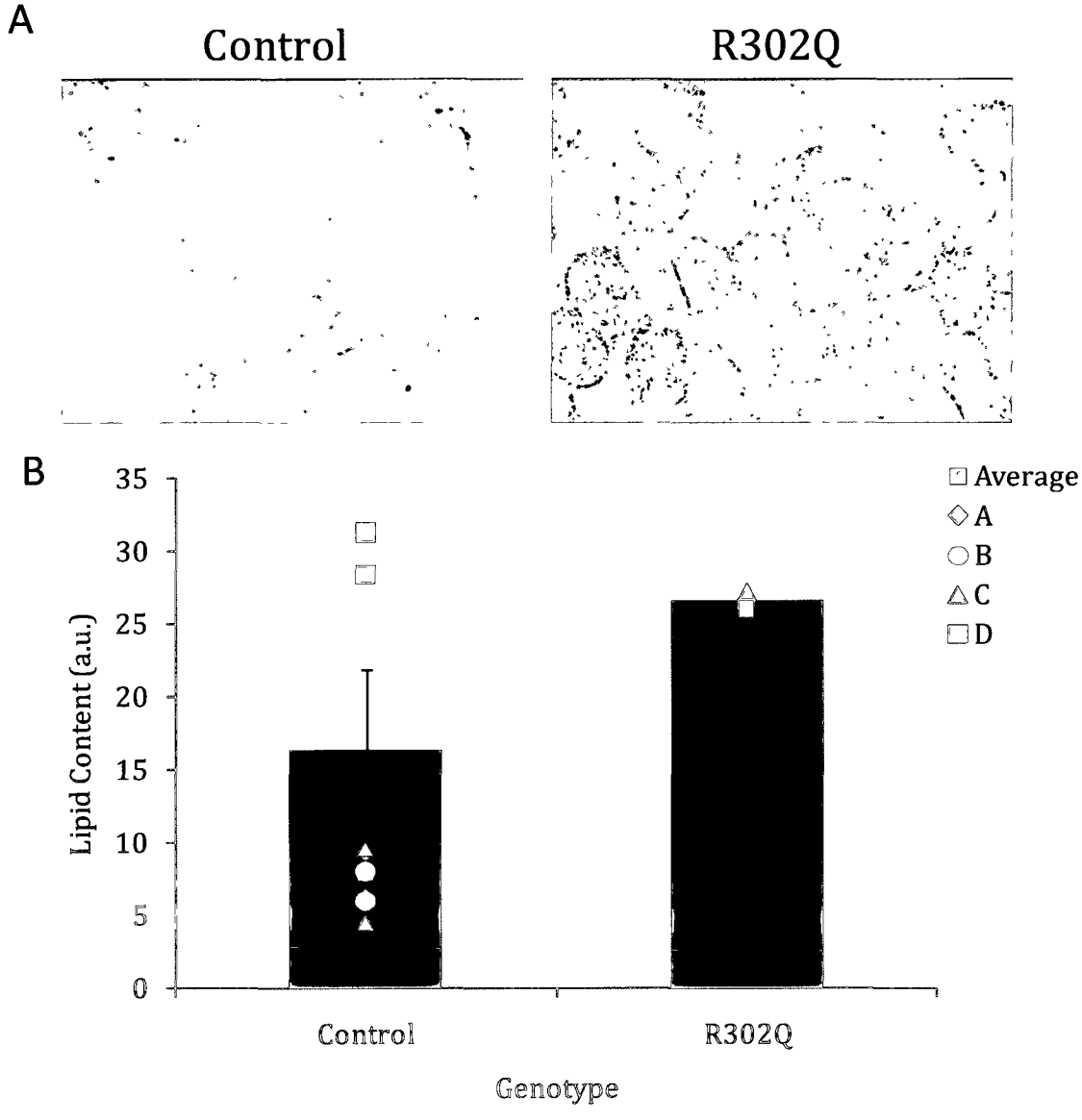
A
Control
R302Q
B
35
30
25
20
15
10
5
0
Lipid Content (a.u.)
Average
A
B
C
D
Control
R302Q
Genotype

for glycogen determinations under identical conditions, but across separate days. Each sample was run alongside its matched control to eliminate effects of day to day variability. Within the population of affected cells, there was a trend for increased glycogen storage (Figure 9). The variability within the affected population is great, however closer analysis of the individual samples reveals that this can be attributed to the highly active individual (D). When 'D' is excluded from the data, the remaining affected subjects show a significant increase in glycogen content compared to their matched control subjects (unpaired, one-tailed t-test; p=0.05).

The control by AMPK over glycogen storage is mostly at the point of glycogen synthesis, as described within the Introduction (see "Targets of AMPK" in the Introduction). Western blot determinations were undertaken to assess changes in GS phosphorylation as mediated by AMPK activity. There was a trend for decreased GS phosphorylation in the affected patients, but no difference in GS expression (Figure 9 B).

Lipid Storage

Addition of a fatty acid, oleate allows one to observe how the cells will differently respond to the new fuel. Circulating fatty acids after a meal are around 200nM in the blood, we assessed various concentrations centering about the physiological value, and determined that 200nM was sufficient for increased TG synthesis, and was readily measurable using techniques available (data not shown).

Between the two subject groups, there was a slight disparity in untreated cells that were not exposed to fatty acids (Figure 10). The affected group exhibited an

Figure 9. Glycogen Content of Cultured Primary Muscle Cells. A) Relative glycogen content as standardized to protein content. Scatter points indicate individual patient measurements grouped by matched control and affected subject. Mean +/- SEM; n:3;. B) Relative content of phosphorylated glycogen synthase (p-GS)and glycogen synthase (GS) measured by integrated density. P-GS standardized to total GS content (c:control; a:R302Q). Mean +/- SEM; n:5,3; p=0.10 by one-tailed unpaired t-test. GS standardized to β-actin loading control. Mean +/- SEM; n:5,3.

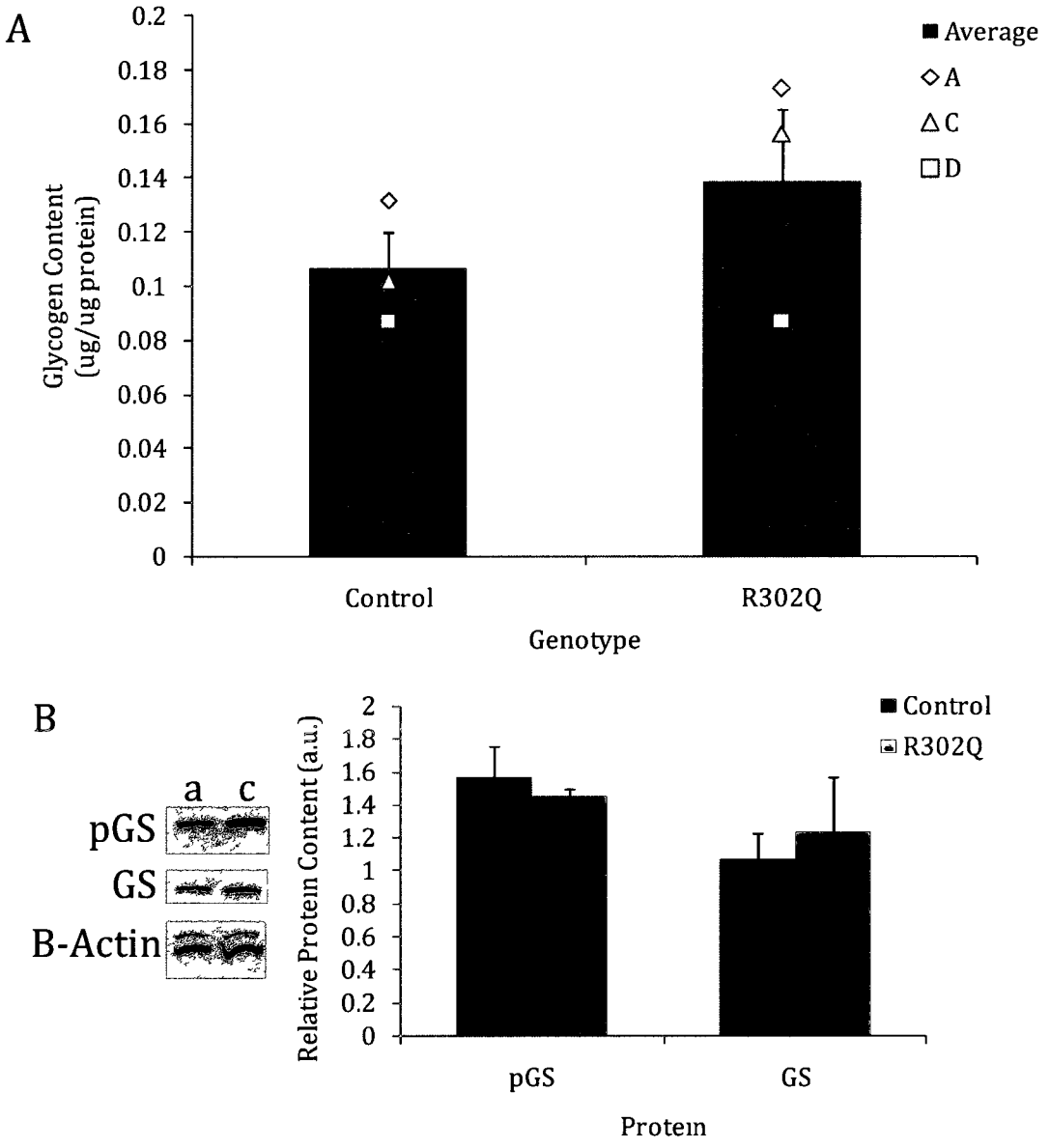
A
0.2
0.18
0.16
0.14
0.12
0.1
0.08
0.06
0.04
0.02
0
Glycogen Content (ug/ug protein)
Average
A
C
D
Control
R302Q
Genotype
B
a
c
pGS
GS
B-Actin
Relative Protein Content (a.u.)
2
1.8
1.6
1.4
1.2
1
0.8
0.6
0.4
0.2
0
Control
R302Q
pGS
GS
Protein

Figure 10. Triglyceride Content of Cultured Primary Muscle Cells. Triglyceride content as normalized to protein content in oleate treated (200nM) and untreated (vehicle) cells. Mean +/- SEM; n:3; $p>0.05$ with a one tailed, unpaired t-test.

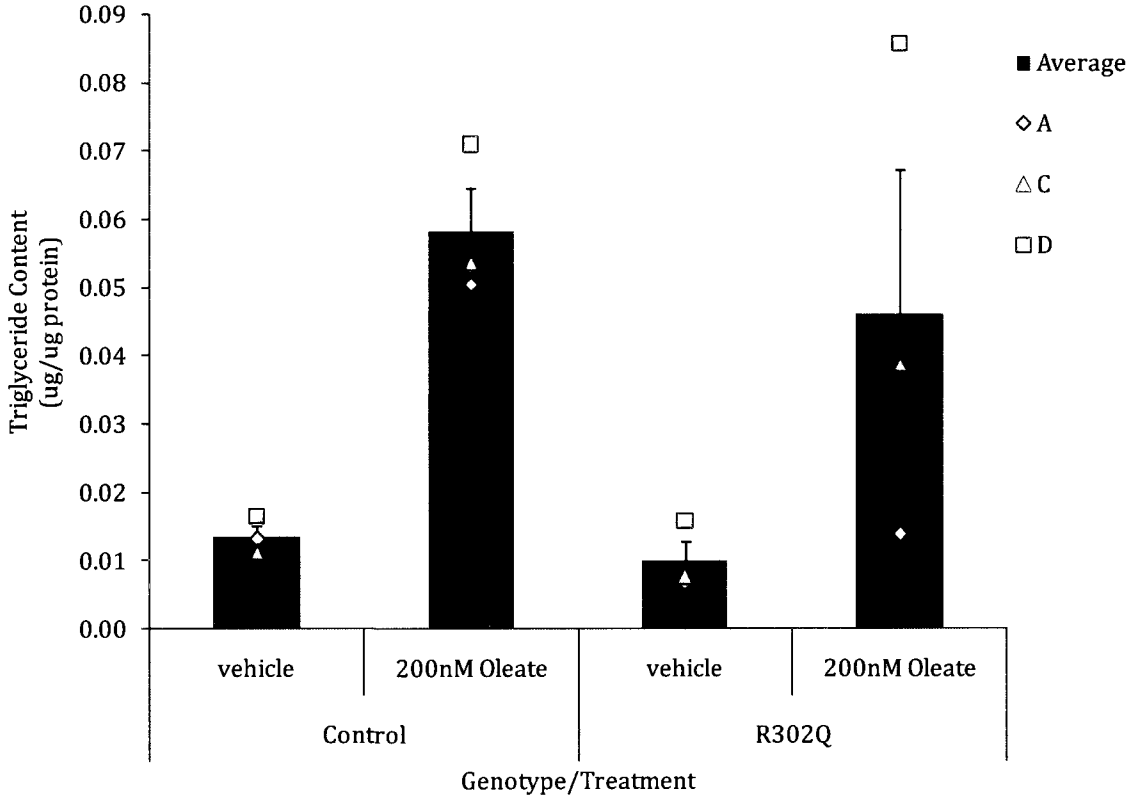
0.09
0.08
0.07
0.06
0.05
0.04
0.03
0.02
0.01
0.00
Triglyceride Content (ug/ug protein)
Average
A
C
D
vehicle
200nM Oleate
vehicle
200nM Oleate
Control
R302Q
Genotype/Treatment

insignificant trend towards decreased basal TG levels. Administration of 200nM oleate resulted in a significant increase in cellular TG. Again, the affected subjects exhibited a high degree of variability. Exclusion of the highly active individuals yielded a significant decrease in TG storage in fatty acid treated cells of affected subjects (unpaired, one-tailed t-test; p:0.01).

Protein Expression

Mitochondrial content can also be modulated through the AMPK regulation system. Expression levels of the Core 1 subunit of Complex III of the electron transport chain was used as a proxy measure of the mitochondrial content of cells. There was a trend for increased Core 1 protein expression, which would be consistent with a conclusion of increased mitochondrial content, in the cells of affected subjects (Figure 11).

AMPK Activity

Optimization of the SAMS peptide assay took several months, and still contains a high degree of variability. To mitigate day to day variability each sample was repeated on at least 3 experiment days; gross outliers and samples that did not respond to AMP stimulation were excluded. In Figure 12A, one can see increased AMPK activity with AMP stimulation in both patient groups. The controls for patient B were included, again to counteract high variability, although B himself was not able to undergo this procedure. While not significant, there was a trend for decreased basal and AMP stimulated activity in the affected AMPK samples. Expansion of the data displaying the

Figure 11. Mitochondrial Content of Cultured Human Primary Myotubes. Protein expression of the Core1 subunit of the electron transport chain Complex III normalized to β-actin loading control and measured by integrated density (c:control; a:R302Q). Mean +/- SEM; n:5,3; p=0.20 with a one tailed, unpaired t-test.

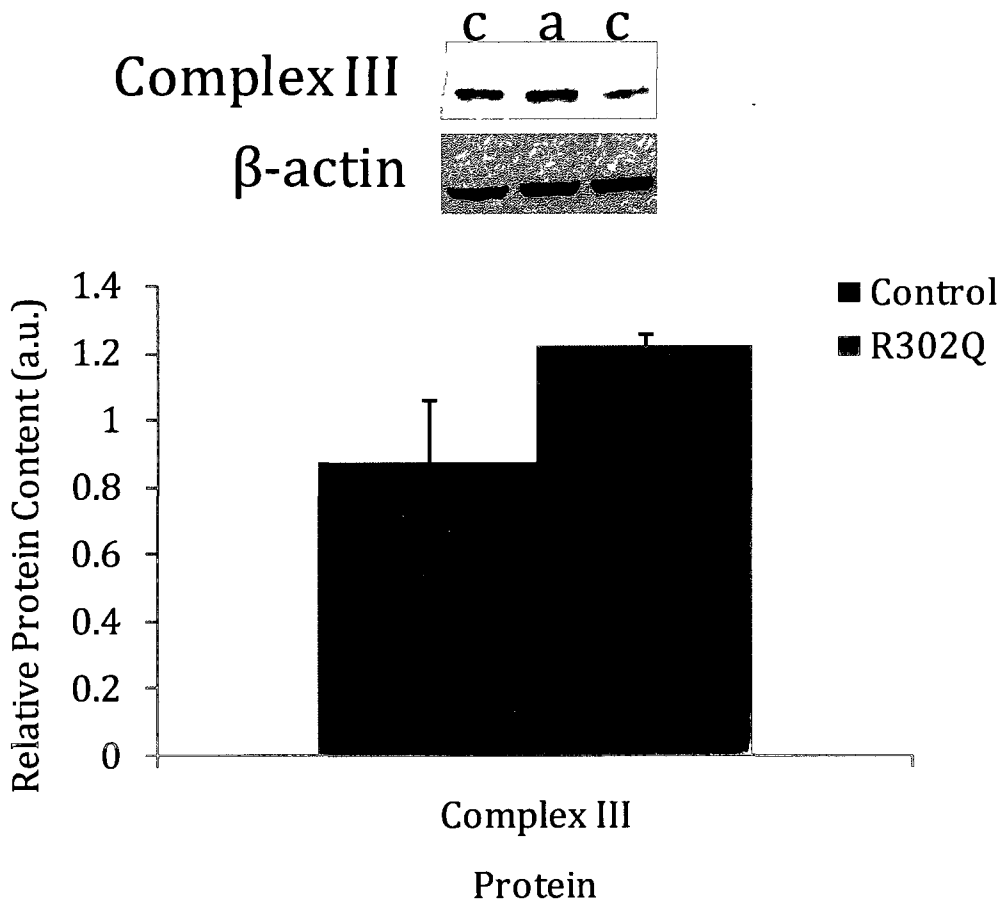
c a c
Complex III
β-actin
1.4
1.2
1
0.8
0.6
0.4
0.2
0
Relative Protein Content (a.u.)
Control
R302Q
Complex III
Protein

Figure 12. AMPK activity. A) AMPK activity as measured by SAMS peptide assay. Purple bars indicate averaged activity, scatter points are averaged values from matched controls and affected subjects. Mean +/- SEM; n: 8,3; Basal p: 0.08 unpaired, one tailed t-test; Activated p=0.1 unpaired, one tailed t-test. B) Scatter points indicate individual highly varied measurements, purple outline indicates average activity. C) Western blot analysis of phosphorylation status of AMPK and ACC. Phospho-proteins standardized to corresponding total expression, total content standardized to β-actin loading control as measured by integrated density (c:control, a:R302Q). Mean +/- SEM; n: 5,3; p-AMPK p=0.074 for one tailed, unpaired t-test; AMPK p=0.199 for one tailed, unpaired t-test.

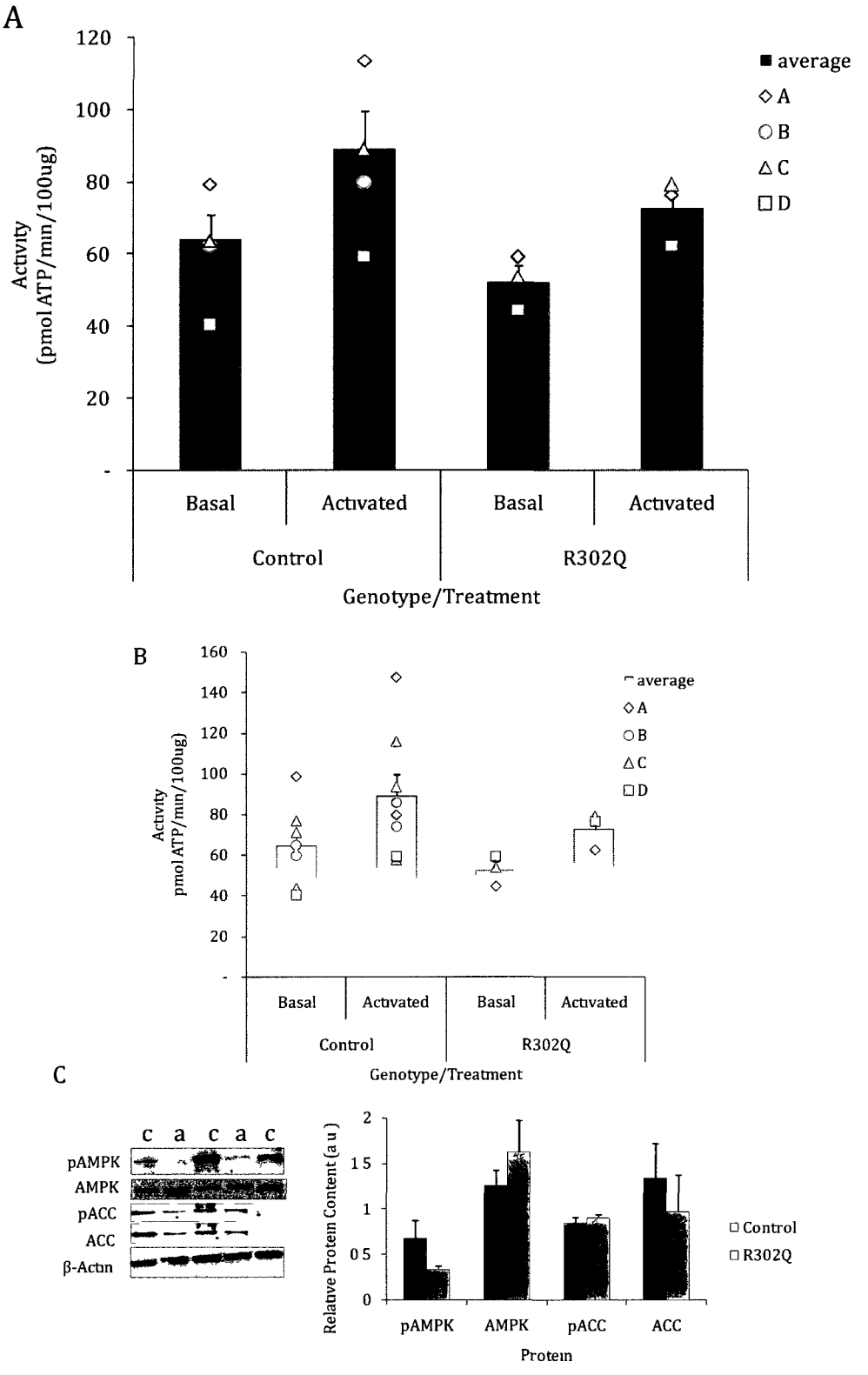
A
120
100
80
60
40
20
-
Activity
(pmol ATP/min/100ug)
average
A
B
C
D
Basal
Activated
Basal
Activated
Control
R302Q
Genotype/Treatment
B
160
140
120
100
80
60
40
20
-
Activity
pmol ATP/min/100ug)
average
A
B
C
D
Basal
Activated
Basal
Activated
Control
R302Q
Genotype/Treatment
C
c a c a c
pAMPK
AMPK
pACC
ACC
β-Actin
2
1 5
1
0 5
0
Relative Protein Content (a u)
pAMPK
AMPK
pACC
ACC
Protein
Control
R302Q

AMPK activities of samples from different subjects revealed some of the substantial variation that was apparently unavoidable (Figure 12B).

A proxy measurement of AMPK activity can be conducted by immunoblot to assess levels of phospho-AMPK and ACC, relative to their total content. Such measurements revealed a striking trend for decreased p-AMPK levels in the affected patients compared to those of matched controls (Figure 12C). Total AMPK levels also appeared to be altered with an inverse effect – the R302Q variants expressing a trend for higher levels of AMPK than their wild-type controls (Figure 12C). Though ACC phosphorylation, was unchanged between the two patient groups, a slight trend for decreased total ACC content was apparent (Figure 12C).

C2C12 Adenovirus System

Adenoviral Infection

The C2C12 mouse muscle cell line is relatively hardy and easy to maintain. It was utilized as a corollary experimental model for our human muscle experiments into the metabolic effects of the γ2 R302Q mutation.

Adenovirus purchased from the University of Alberta expressed both GFP and one of either human WTγ2 or the R302Q variant. GFP expression allowed us to measure viral uptake and distribution in cultured cells using fluorescence microscopy (Figure 13). Various MOIs were used to determine the ideal conditions to achieve maximal viral uptake and expression within the cells, and to ensure equal protein

Figure 13. Adenoviral Infected C2C12 Myotubes. Images taken from 6 day differentiated cells after 48 hours of incubation with either γ2 WT (MOI:100), or γ2 R302Q (MOI:150) adenovirus. Light exposures for 2s, fluorescent exposure for GFP for 15s.

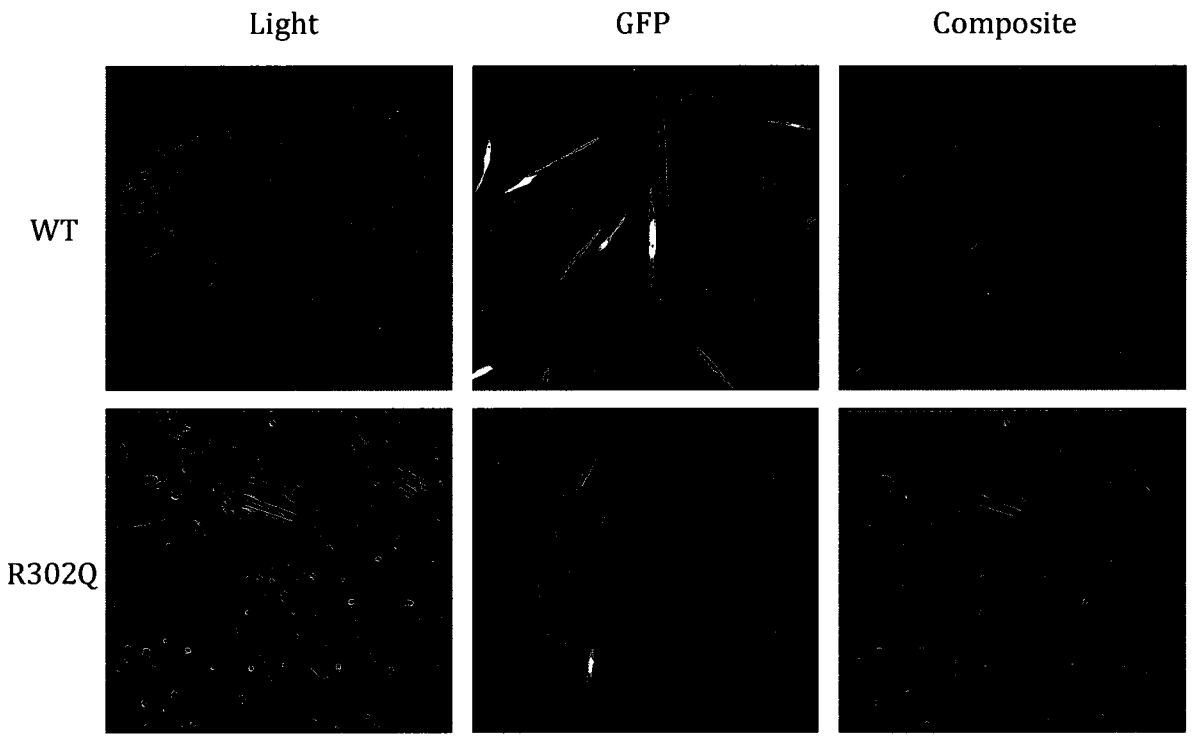
Light
GFP
Composite
WT
R302Q

expression between the two different viral strains. Cells were then differientiated for 6 days; adenoviral addition did not hinder differentiation.

Carbohydrate Storage

Glycogen storage was measured in the infected cells, as well as the vehicle treated control cells. No differences were observed between the three groups (Figure 14A), though glycogen levels were extremely low.

Lipid Storage

Similar to the human primary myotubes, the C2C12 cells were treated with either 2% BSA differentiation media with or without the addition of fatty acid to stimulate TG production. While there was a clear increase in TG levels with the addition of 200nM oleate to the differentiation media, there was no difference between the different groups (Figure 14B).

Protein Expression

GFP levels were equal in the adenoviral groups, with none detectable in vehicle treated control cells (Figure 15). AMPK content was not significantly changed in either viral group, however no p-AMPK was detectable in any of the samples (Figure 15). As a proxy measure of AMPK activity, ACC phosphorylation was also measured, with no difference seen between the groups. No changes were evident in comparisons of levels of p-GS, GS, or Complex III (Figure 15).

Figure 14. Fuel Storage within C2C12 Myotubes. A) Glycogen content of C2C12 cells incubated with or without WT or R302Q viroids normalized to protein content. Mean +/- SEM; n:3; $p>0.05$ with a one way ANOVA. B) Triglyceride content of C2C12 cells incubated with or without viroids, with or without the addition of 200nM oleate and normalized to protein content. Mean +/- s.e.m; n:3; $p>0.05$ with a one way ANOVA.

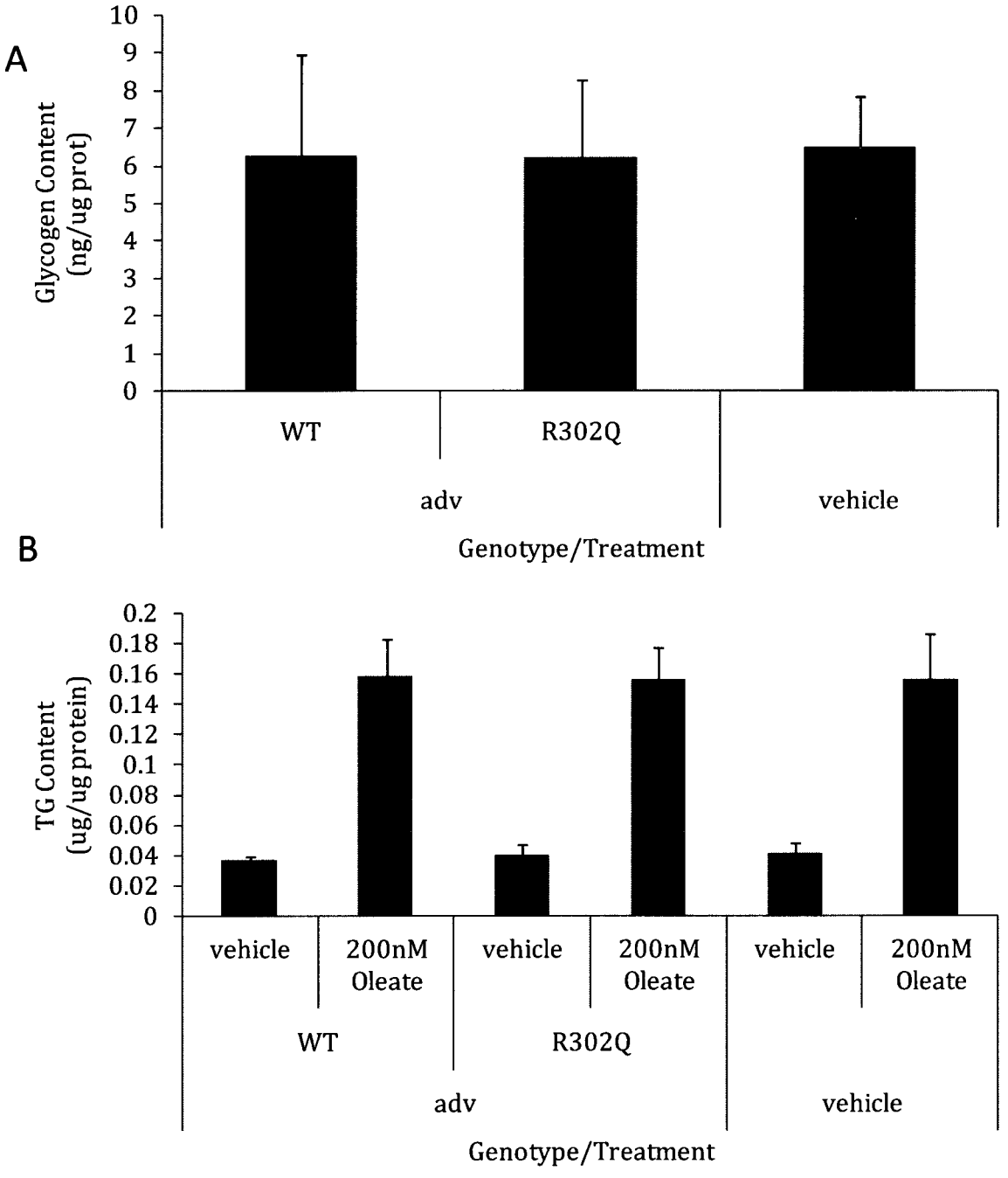
A
Glycogen Content (ng/ug prot)
10
9
8
7
6
5
4
3
2
1
0
WT
R302Q
adv
vehicle
Genotype/Treatment
B
TG Content (ug/ug protein)
0.2
0.18
0.16
0.14
0.12
0.1
0.08
0.06
0.04
0.02
0
vehicle
200nM Oleate
vehicle
200nM Oleate
vehicle
200nM Oleate
WT
R302Q
adv
vehicle
Genotype/Treatment

Figure 15. Protein Expression within C2C12 Myotubes. Protein collected from C2C12 cells incubated with or without WT or R302Q viroids. Western blot analyses of phospho-proteins and their total protein counterparts. Phospho-proteins standardized to corresponding total expression, total protein content normalized to β-actin loading control as measured by integrated density. Mean +/- SEM; n:3; $p>0.05$ for all proteins.

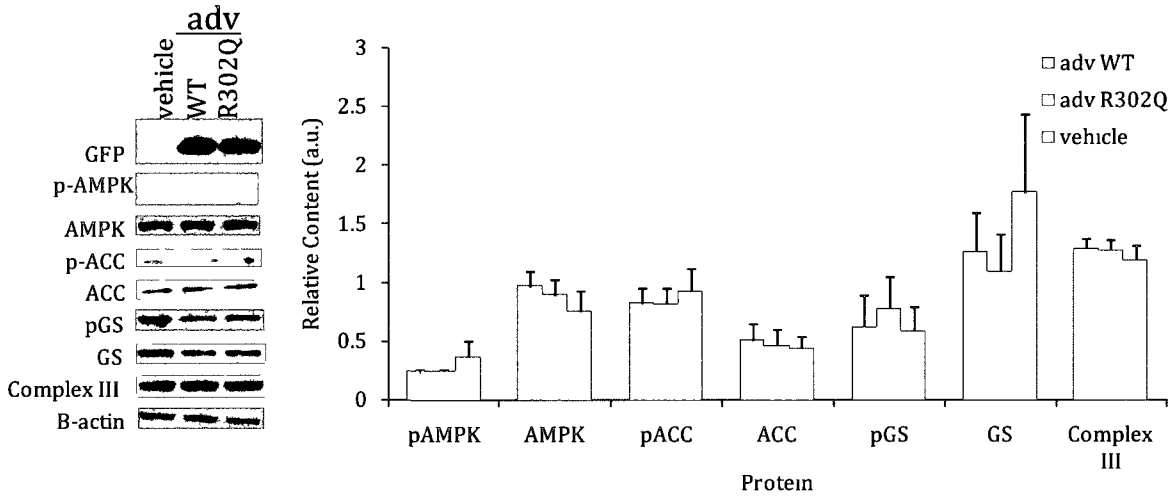
adv
vehicle
WT
R302Q
GFP
p-AMPK
AMPK
p-ACC
ACC
pGS
GS
Complex III
B-actin
Relative Content (a.u.)
3
2.5
2
1.5
1
0.5
0
adv WT
adv R302Q
vehicle
pAMPK
AMPK
pACC
ACC
pGS
GS
Complex III
Protein

Discussion

AMPK acts as an important regulator of energy levels within the cell and organism. When activated by increased AMP:ATP resulting from fuel depletion, and other cellular stresses, it works to restore fuel levels. Directly binding either AMP or ATP, AMPK activity is modulated by conformational changes and phosphorylation status. Bound AMP initially increases overall activity modestly, subsequently allowing for phosphorylation by upstream kinases and protection against deactivating phosphatases resulting in a sharp and rapid increase in AMPK activity. By directly inhibiting ATP consuming synthetic pathways, and stimulating ATP producing degradation pathways, AMPK can quickly restore energy balance (reviewed in (53, 125, 144)).

Studies of AMPK γ Isoform Mutations

Mutations within the γ subunits result in alterations in AMPK activity and subsequent fuel storage abnormalities (reviewed in (46, 53, 125, 144)). Skeletal muscle specific mutations in the γ3 isoform are well characterized for their impact on metabolism and AMPK activity. Studies into the R225Q mutation in RN^- pigs revealed that this was a gain-of-function impact resulting in increased glycogen storage and enhanced endurance exercise capacity (49, 52, 83, 95). A homologous mutation in human subjects, the γ3 R225W variant, similarly resulted in augmented AMPK activity, increased glycogen storage within skeletal muscle and resistance to fatigue (31, 32). Since the γ2 R302Q mutation is located in the same location as the R225Q mutation in the γ3 subunit, we anticipated similar outcomes in our R302Q mutant-tissues and cells.

The R302Q mutation of the human γ2 subunit, results in the development of WPW syndrome, a cardiomyopathy characterized by gross accumulation of glycogen and impaired electrical conductance (91). Early *in vivo* studies demonstrated a decrease in glucose uptake, as measured by positron emission tomography (PET) analysis of ^{18}F-fluoro-deoxy glucose (FDG) uptake within human myocardium, consistent with impaired AMPK activity (51). However, the conclusions of the latter study could have been confounded by the effects of cardiomyopathy (*e.g.*, scarring, hypertrophy caused by excessive glycogen content).

Transgenic mouse models have been developed to express the human WT γ2 subunit and the γ2 R302Q variant (119). Measurements of AMPK activity on immunopurified AMPK from heart tissue (using the SAMS peptide assay) from the R302Q transgenic mouse model led to the conclusion that the R302Q variant is a loss-of-function mutation resulting in diminished AMPK activity (119). However, analysis of primary cardiomyocytes obtained from the transgenic mice yielded findings consistent with enhanced AMPK and accelerated glycogen synthesis (38, 94). Using an adenoviral vector to express human WT or the R302Q variant of γ2, Folmes et al. (38) were able to directly measure AMPK activity and confirm an increase in the R302Q expressing cultured cardiomyocytes. Much of the controversy within the literature could be attributable to methods of normalizing the data. Many earlier reports directly measured AMPK activity as normalized to total heart weight. As the R302Q variant results in a disproportionally enlarged glycogen rich heart that could artificially lower measurements of activity (119). Studies where activity is normalized to total protein, alternatively, report an increase in AMPK activity in R302Q expressing samples,

perhaps a more accurate measurement (38). Even within individual studies, measurements of AMPK activity normalized to heart weight, versus measurements normalized to cellular protein content yield opposite results (38). Analysis of a similar γ2 mutation, T400N, expressed in transgenic mice resulted in a biphasic effect of γ2 on cardiac muscle AMPK activity as measured on immunopurified total AMPK (using the SAMS peptide assay), with increased activity in samples from young mice but reduced activity later in life (12). Levels of glycogen content are greatly increased in the mouse R302Q expressing heart (119).

Skeletal muscle biopsies of affected subjects allowed us to explore the impact of the mutation *in vitro*. Using biopsies obtained from the *vastus lateralis* of affected and matched control subjects, we hoped to elucidate the impact of the R302Q mutation on the AMPK signalling pathway and skeletal muscle metabolism by examining various targets of AMPK. Despite a small sample size, the outcomes of our various experiments, combined, allow us to put forth a revised model for γ2 function in skeletal muscle (see below). Initially we hypothesized that the R302Q mutation would impact AMPK activity and skeletal muscle metabolism in a similar manner to the γ3 mutations discussed (see "AMPK in Health and Disease" in the Introduction). Our results, however, do not generally support this hypothesis.

Analysis of *Ex Vivo* Samples

In the *ex vivo* histology of *vastus lateralis* samples there was no difference between the subject groups in fibre type ratio, or glycogen content. The proportion of the three different three major fibre types were comparable to literature values (124).

Glycogen content results were highly variable. At least some of the variability would be attributable to freezing technique. In the first few samples, ice crystals developed during the freezing of the muscle; this punctured the fiber structure, and made analysis difficult. For analysis, these regions were avoided, and those regions between the crystals were selected. However, this proved challenging as some samples were far too perforated to find regions large enough to reliably measure. Subsequent samples, after more experience with the technique, did not yield the same level of ice crystal formation and were much more readily analyzed. Despite improvements in tissue freezing, there was no apparent difference in glycogen content between affected and control subjects. Factors that are known to affect muscle glycogen storage include exercise and feeding state (*e.g.*, fed *vs.* fasted). All subjects were asked to abstain from physical exercise for 48 h prior to the procedure, including climbing stairs on the morning of the biopsy to minimize glycogen depletion. In addition, subjects fasted for 12h prior to biopsy to normalize circulating glucose levels. Studies analyzing *ex vivo* glycogen content within groups expressing the γ3 R225W mutation demonstrated a doubling of levels in the affected subjects compared to matched control subjects (31). Our observation of unchanged glycogen content could be due to small sample size, or to the possibility that the γ2 subunit has little effect of skeletal muscle glycogen content.

However, a striking phenotype was found during analysis of *vastus lateralis* IMCL. Oil red O stains neutral lipid deposits, allowing for measurements of the levels of triglycerides and other neutral lipids within the *ex vivo* samples. A significant increase in lipid content was evident in the affected subjects compared to all control subjects ($p=0.0015$). Interestingly, the highly active individuals (D, D1, and D2) exhibited

consistently elevated lipid content; higher muscle triglyceride levels have been previously reported in skeletal muscle of physically active individuals (66). Notably, the remaining affected individual (C), who has more average activity levels, had almost identical lipid content to the other highly trained affected subject. This striking increase in lipid content within the muscle fibres, suggests a possible increase in AMPK activity through augmented fatty acid uptake; though this observation could also be the result of decreased AMPK activity resulting in decreased lipid degradation pathways such as β-oxidation. Samples of only two affected subjects were able to be analyzed, statistical comparisons between the affected subjects and their matched control subjects suggested only a trend for increased lipid content ($p=0.07$). So while the initial analysis of lipid content suggest a strong difference, more samples are needed to confirm this observation.

In Vitro Primary Myocyte Determinations

Generally, *ex vivo* histological analyses are an excellent tool, as they offer a snapshot of the *in vivo* environment; however, such analyses also have significant limitations. Skeletal muscle fuel storage is controlled by many neurohormonal factors (such as insulin, adiponectin, etc.). While subjects were generally well rested and fasting at the time of muscle biopsy, the levels of such neurohormonal factors may be highly variable. This can make histology a double-edged sword, on one hand allowing for a more representative look at the condition within a cell in its natural environment, but also subject to many variables that cannot be controlled.

The isolation of satellite cells from muscle allows one to examine the biochemical pathways within the muscle cells *in vitro*, while maintaining complete

control over the environment. Thus, one can glean the contributions of internal components without the complicating effects of external effectors, with the caveat that this model system will never be completely representative of the tissue *in vivo*. Though, several studies have shown that determinations made in primary cell culture correlate well with corresponding *in vivo* determinations, making cultured cells a powerful tool for controlled mechanistic studies (44, 132). Satellite cells from each individual were grown under identical glucose, amino acid, and growth factor conditions, with the aim of isolating the effects of the γ2 mutation.

Interestingly, differences in fuel storage became more apparent with the *in vitro* cell culture determinations. There was a trend for increased glycogen storage, in the R302Q expressing cells. With the exclusion of the highly active subjects, a significant increase in glycogen content within the cells of R302Q subjects compared to the cells of control subjects was observed. Notably, our values were comparable to those reported in the literature (6). As discussed previously (see "Targets of AMPK" in the Introduction), glycogen content reflects a dynamic process of synthesis by GS and degradation by GP. Allosteric activators, inhibitors and signalling enzymes converge upon GS and GP to ensure the appropriate amount of glycogen is being stored and mobilized. Thus, by measuring glycogen content alone, it is not possible to assess which aspect of its metabolism is affected. Increased glycogen could indicate decreased GS inhibition from direct AMPK phosphorylation suggesting a loss of AMPK function, or increased G6P accumulation – from augmented GLUT4/hexokinase activity – suggesting a gain of AMPK function. The phosphorylation status of GS was not significantly different in the affected subjects, though there may be a trend for a

decrease, suggesting a loss of AMPK activity within the cell. Since direct measurements of glucose uptake were not made, it is difficult to unequivocally describe the impact of AMPK on glycogen storage with this data alone.

A second important source of stored fuel in skeletal muscle is triglyceride. AMPK promotes fatty acid catabolism, while anabolic pathways are inhibited. Resting muscle cells in differentiation medium do not accumulate vast amounts of triglyceride as skeletal muscle cells are incapable of engaging in *de novo* lipid synthesis. Moreover the DMEM medium provides glucose but no lipidic substrates. To assess the impact of the mutation on lipid metabolism we therefore incubated cells in the presence of oleate. When AMPK is activated it inhibits triglyceride synthesis, and favours β-oxidation for replenishment of ATP stores. A slight trend for decreased basal and oleate-treated levels of triglyceride was seen in the R302Q subjects. Similar to glycogen content, cellular triglyceride levels are maintained by a tight equilibrium between lipid synthesis and oxidation. More importantly, lipid homeostasis is regulated by AMPK at various points (see "Targets of AMPK" in the Introduction). Decreased triglyceride content could indicate enhanced AMPK activity leading to increased β-oxidation, or could indicate a decrease in FAT/CD36 mediated fatty acid uptake. As the cells were grown in a lipid-free media prior to fatty acid treatment, it is possible that fatty acid transport was already downregulated. Theoretically, decreased fatty acid uptake, from reduced AMPK activity, could account for decreased fatty acid provisioning for triglyceride synthesis, leading to decreased triglyceride levels within the R302Q expressing cells. Finally, mitochondrial content, as measured by expression of the Core1 subunit of Complex III, was unchanged in the myotubes of affected

subjects (p=0.20). Additional mitochondrial proteins could be measured to corroborate these results, or cellular mitochondrial content could be analyzed with the use of mitochondrial-specific dyes, such as Mitotracker green (Molecular Probes).

Levels of the γ2 subunit are thought to be relatively low in skeletal muscle, with the γ3 isoform accounting for the majority of the AMPK activity. While the mRNA of γ2 is known to be expressed in skeletal muscle (28), it is not known what levels of γ2 protein is expressed. The fundamental source of this controversy is the absence of a specific AMPK γ2 antibody. We attempted to assess the levels of the three γ isoforms; unfortunately, it appeared that all three antibodies reacted only with the γ1 isoform, making comparisons impossible (data not shown). Even so, we would anticipate that if the γ2 isoform were present, it would be at a much lower level than the skeletal muscle specific γ3. As such, we would expect the impact of the R302Q mutation to be moderate, and only direct effects of AMPK would likely be relevant (*e.g.* phosphorylation of targets, and inhibition of synthesis pathways). Though one cannot rule out a possible effect of the mutation on complex assembly, work would need to be done to assess whether the R302Q mutation can disrupt complex formation, and alter isoform preference.

Direct measurements of AMPK activity *in vitro* may offer the best insight into the impact of the R302Q mutation. The SAMS peptide assay allows for direct measurements of basal and AMP-activated AMPK activity. The use of the engineered SAMS peptide allows for specific measurements of AMPK activity as it is a specific target. There are many difficulties surrounding AMPK measurements of activity, however. While the SAMS peptide is used to detect AMPK specific activity, as opposed

to general kinase action, phosphatases as well as small cellular molecules such as AMP and ATP within the sample can interfere. We attempted to circumvent these problems by purifying total AMPK from each sample as well as by including various phosphatase inhibitors. AMPK α1 and α2 antibodies were then used together to isolate total AMPK from a fixed amount of sample.

While the AMPK activity assay can lead to highly variable results, many repetitions and the inclusion of extra control samples helped to diminish the variability. Within the affected population, both the basal and AMP activated rates showed a trend for decreased activity, though this did not reach significance. Within the literature, there is a wide variety of measured activity levels for AMPK (113, 146, 149). Each study uses slightly different conditions or isolation techniques, with some purifying AMPK through immunoprecipitation, and others using recombinant AMPK or using impure whole cell lysate. However our measured AMPK activity levels are within the range of published values, and comparable to studies using similar techniques (149).

Examination of indirect indicators of AMPK activity yielded interesting results. While the phosphorylation status of ACC, a direct target of AMPK, was unchanged, phosphorylation of AMPK itself was decreased in the affected population compared to their controls ($p=0.07$), while AMPK content was unchanged ($p>0.1$). A decrease in p-AMPK levels could indicate an impairment of AMP's ability to protect the α subunit from dephosphorylation through binding of the γ subunit, suggestive of impaired AMP binding within the mutated CBS1 region.

The C2C12 Adenoviral System

Adenoviral infection of C2C12 cells with either the human γ2 subunit or the R302Q variant was intended to corroborate results observed in the human samples with the advantage of a genetically identical background. Unfortunately, limitations of the model resulted in no observable differences between the groups within any of the factors measured. This was likely due to a limited ability of the cells to uptake the virus. Regardless of MOI tested, the maximal cellular uptake was around 5% of the cells, as measured by fluorescence microscopy for GFP expression. In fact, the C2C12 cell line is known to be particularly resistant to viral uptake (69, 82). However, the concept behind the system is still strong, as a genetically controlled cell line is ideal for determining the specific contribution of the R302Q mutation. Thus future work should be attempted using an alternative cell culture line. Primary mouse myoblasts could offer a strong corollary to the human primary samples. Use of inbred mouse strains would minimize individual variability. Another advantage of primary myocytes over immortalized cell lines is an absence of alterations attributable to immortalization, which could impact a variety of cellular pathways, and result in a less representative model for human metabolism.

Major Findings

The most striking finding of this research was the apparent decrease in basal and AMP activated activity in cells from affected individuals as measured using both the SAMS peptide assay and the p-AMPK/AMPK levels. With trends apparent in levels of fuel storage within *ex vivo* and *in vitro* analysis of muscle tissue.

These data taken together lead to conflicting interpretations. Direct measures of AMPK activity, through the SAMS peptide assay, and p-AMPK levels, suggest decreased

AMPK activity within the cell, however, observations of fuel storage can lead to opposing conclusions. Taken in the light of each aspect of fuel storage – synthesis and degradation – a compelling model emerges.

Decreased AMPK activity could contribute to increased glycogen synthesis through an inability to appropriately inhibit GS while glucose enters the cell through alternative pathways (*e.g.* GLUT1, insulin-stimulated GLUT4). The observed trend for decreased TG storage in the affected cells can also be correlated to decreased AMPK activity. TG synthesis requires the uptake of fatty acids to be incorporated into TG molecules. AMPK-mediated control of fatty acid uptake could be mediated through the FAT/CD36 transporter system (75, 104). Decreased AMPK activity could impair fatty acid uptake, limiting substrate availability for TG synthesis resulting in the decrease in triglyceride content observed in our affected population. Each of these fuel storage observations should be confirmed in further studies with analysis of basal glucose and fatty acid uptake within the two genotype groups.

As compelling as some of these conclusions may be, one must bear in mind that the sample size used to examine these various metabolic pathways was extremely small. Recruitment of multiple matched control subjects for each of our affected subjects could help reduce the effects of variability within the control population. However, it does not mitigate the fact that only four samples from affected patients were obtained and only three of these could be used for analysis of the R302Q mutation. The large range in age and activity level within the affected subject group further adds to the variability within the group. Future work on this project will need to focus on the recruitment of more affected individuals in order to obtain statistical

power. Thus, it is difficult to draw significant conclusions from the data at present. With this important caveat, a tentative model will be proposed.

Proposed Mechanism

Much controversy exists over the nature of the R302Q mutation and whether it results in a gain of function (38), or loss of function (51, 119), though more recent studies support the idea of it being a gain of function similar to the γ3 mutations studied (38). However, a loss of function of AMPK could also contribute to increased glycogen content within the cell resulting from an inability to appropriately inhibit glycogen synthesis during times of energy depletion.

From observations obtained from skeletal muscle we can infer the impact of the R302Q mutation on heart metabolism. We propose that the AMPKγ2 R302Q mutation contributes to the development of WPW in human populations through impairment of AMPK activity. Similar to the results we have seen in skeletal muscle, we would anticipate that decreased AMPK activity impairs its ability to effectively inhibit GS activity leading to the excessive accumulation of glycogen within the heart, in turn resulting in the development of WPW syndrome. As the γ2 subunit is only moderately expressed in skeletal muscle its impact on skeletal muscle metabolism would be less severe, resulting in increased lipid and glycogen storage within the cell, and potentially decreased mitochondrial content.

References

1. **Abu-Elheiga, L., W. R. Brinkley, L. Zhong, S. S. Chirala, G. Woldegiorgis, and S. J. Wakil.** 2000. The subcellular localization of acetyl-CoA carboxylase 2. Proc Natl Acad Sci U S A **97:**1444-9.
2. **Abu-Elheiga, L., A. Jayakumar, A. Baldini, S. S. Chirala, and S. J. Wakil.** 1995. Human acetyl-CoA carboxylase: characterization, molecular cloning, and evidence for two isoforms. Proc Natl Acad Sci U S A **92:**4011-5.
3. **Abu-Elheiga, L., M. M. Matzuk, K. A. Abo-Hashema, and S. J. Wakil.** 2001. Continuous fatty acid oxidation and reduced fat storage in mice lacking acetyl-CoA carboxylase 2. Science **291:**2613-6.
4. **Abu-Elheiga, L., W. Oh, P. Kordari, and S. J. Wakil.** 2003. Acetyl-CoA carboxylase 2 mutant mice are protected against obesity and diabetes induced by high-fat/high-carbohydrate diets. Proc Natl Acad Sci U S A **100:**10207-12.
5. **Ahmad, F., M. Arad, N. Musi, H. He, C. Wolf, D. Branco, A. R. Perez-Atayde, D. Stapleton, D. Bali, Y. Xing, R. Tian, L. J. Goodyear, C. I. Berul, J. S. Ingwall, C. E. Seidman, and J. G. Seidman.** 2005. Increased alpha2 subunit-associated AMPK activity and PRKAG2 cardiomyopathy. Circulation **112:**3140-8.
6. **Al-Khalili, L., M. Forsgren, K. Kannisto, J. R. Zierath, F. Lonnqvist, and A. Krook.** 2005. Enhanced insulin-stimulated glycogen synthesis in response to insulin, metformin or rosiglitazone is associated with increased mRNA expression of GLUT4 and peroxisomal proliferator activator receptor gamma co-activator 1. Diabetologia **48:**1173-9.
7. **Amodeo, G. A., M. J. Rudolph, and L. Tong.** 2007. Crystal structure of the heterotrimer core of Saccharomyces cerevisiae AMPK homologue SNF1. Nature **449:**492-5.
8. **Andersson, U., K. Filipsson, C. R. Abbott, A. Woods, K. Smith, S. R. Bloom, D. Carling, and C. J. Small.** 2004. AMP-activated protein kinase plays a role in the control of food intake. J Biol Chem **279:**12005-8.
9. **Aschenbach, W. G., M. F. Hirshman, N. Fujii, K. Sakamoto, K. F. Howlett, and L. J. Goodyear.** 2002. Effect of AICAR treatment on glycogen metabolism in skeletal muscle. Diabetes **51:**567-73.
10. **Atkinson, D. E.** 1968. The energy charge of the adenylate pool as a regulatory parameter. Interaction with feedback modifiers. Biochemistry **7:**4030-4.
11. **Bandyopadhyay, G. K., J. G. Yu, J. Ofrecio, and J. M. Olefsky.** 2006. Increased malonyl-CoA levels in muscle from obese and type 2 diabetic subjects lead to decreased fatty acid oxidation and increased lipogenesis; thiazolidinedione treatment reverses these defects. Diabetes **55:**2277-85.
12. **Banerjee, S. K., R. Ramani, S. Saba, J. Rager, R. Tian, M. A. Mathier, and F. Ahmad.** 2007. A PRKAG2 mutation causes biphasic changes in myocardial AMPK activity and does not protect against ischemia. Biochem Biophys Res Commun **360:**381-7.
13. **Barnes, B. R., J. W. Ryder, T. L. Steiler, L. G. Fryer, D. Carling, and J. R. Zierath.** 2002. Isoform-specific regulation of 5' AMP-activated protein kinase in

skeletal muscle from obese Zucker (fa/fa) rats in response to contraction. Diabetes **51:**2703-8.

14. **Beg, Z. H., D. W. Allmann, and D. M. Gibson.** 1973. Modulation of 3-hydroxy-3-methylglutaryl coenzyme A reductase activity with cAMP and wth protein fractions of rat liver cytosol. Biochem Biophys Res Commun **54:**1362-9.
15. **Bergeron, R., J. M. Ren, K. S. Cadman, I. K. Moore, P. Perret, M. Pypaert, L. H. Young, C. F. Semenkovich, and G. I. Shulman.** 2001. Chronic activation of AMP kinase results in NRF-1 activation and mitochondrial biogenesis. Am J Physiol Endocrinol Metab **281:**E1340-6.
16. **Besse, A., B. Lamothe, A. D. Campos, W. K. Webster, U. Maddineni, S. C. Lin, H. Wu, and B. G. Darnay.** 2007. TAK1-dependent signaling requires functional interaction with TAB2/TAB3. J Biol Chem **282:**3918-28.
17. **Bianchi, A., J. L. Evans, A. J. Iverson, A. C. Nordlund, T. D. Watts, and L. A. Witters.** 1990. Identification of an isozymic form of acetyl-CoA carboxylase. J Biol Chem **265:**1502-9.
18. **Bolster, D. R., S. J. Crozier, S. R. Kimball, and L. S. Jefferson.** 2002. AMP-activated protein kinase suppresses protein synthesis in rat skeletal muscle through down-regulated mammalian target of rapamycin (mTOR) signaling. J Biol Chem **277:**23977-80.
19. **Bonen, A., A. Chabowski, J. J. Luiken, and J. F. Glatz.** 2007. Is membrane transport of FFA mediated by lipid, protein, or both? Mechanisms and regulation of protein-mediated cellular fatty acid uptake: molecular, biochemical, and physiological evidence. Physiology (Bethesda) **22:**15-29.
20. **Brown, M. S., G. Y. Brunschede, and J. L. Goldstein.** 1975. Inactivation of 3-hydroxy-3-methylglutaryl coenzyme A reductase in vitro. An adenine nucleotide-dependent reaction catalyzed by a factor in human fibroblasts. J Biol Chem **250:**2502-9.
21. **Burwinkel, B., J. W. Scott, C. Buhrer, F. K. van Landeghem, G. F. Cox, C. J. Wilson, D. Grahame Hardie, and M. W. Kilimann.** 2005. Fatal congenital heart glycogenosis caused by a recurrent activating R531Q mutation in the gamma 2-subunit of AMP-activated protein kinase (PRKAG2), not by phosphorylase kinase deficiency. Am J Hum Genet **76:**1034-49.
22. **Carling, D., P. R. Clarke, V. A. Zammit, and D. G. Hardie.** 1989. Purification and characterization of the AMP-activated protein kinase. Copurification of acetyl-CoA carboxylase kinase and 3-hydroxy-3-methylglutaryl-CoA reductase kinase activities. Eur J Biochem **186:**129-36.
23. **Carling, D., and D. G. Hardie.** 1989. The substrate and sequence specificity of the AMP-activated protein kinase. Phosphorylation of glycogen synthase and phosphorylase kinase. Biochim Biophys Acta **1012:**81-6.
24. **Carlson, C. A., and K. H. Kim.** 1973. Regulation of hepatic acetyl coenzyme A carboxylase by phosphorylation and dephosphorylation. J Biol Chem **248:**378-80.
25. **Celenza, J. L., and M. Carlson.** 1986. A yeast gene that is essential for release from glucose repression encodes a protein kinase. Science **233:**1175-80.
26. **Chen, Z., J. Heierhorst, R. J. Mann, K. I. Mitchelhill, B. J. Michell, L. A. Witters, G. S. Lynch, B. E. Kemp, and D. Stapleton.** 1999. Expression of the

AMP-activated protein kinase beta1 and beta2 subunits in skeletal muscle. FEBS Lett **460:**343-8.

27. **Cheung, P. C., A. R. Nebreda, and P. Cohen.** 2004. TAB3, a new binding partner of the protein kinase TAK1. Biochem J **378:**27-34.
28. **Cheung, P. C., I. P. Salt, S. P. Davies, D. G. Hardie, and D. Carling.** 2000. Characterization of AMP-activated protein kinase gamma-subunit isoforms and their role in AMP binding. Biochem J **346 Pt 3:**659-69.
29. **Cool, B., B. Zinker, W. Chiou, L. Kifle, N. Cao, M. Perham, R. Dickinson, A. Adler, G. Gagne, R. Iyengar, G. Zhao, K. Marsh, P. Kym, P. Jung, H. S. Camp, and E. Frevert.** 2006. Identification and characterization of a small molecule AMPK activator that treats key components of type 2 diabetes and the metabolic syndrome. Cell Metab **3:**403-16.
30. **Corton, J. M., J. G. Gillespie, S. A. Hawley, and D. G. Hardie.** 1995. 5-aminoimidazole-4-carboxamide ribonucleoside. A specific method for activating AMP-activated protein kinase in intact cells? Eur J Biochem **229:**558-65.
31. **Costford, S. R., N. Kavaslar, N. Ahituv, S. N. Chaudhry, W. S. Schackwitz, R. Dent, L. A. Pennacchio, R. McPherson, and M. E. Harper.** 2007. Gain-of-function R225W mutation in human AMPKgamma(3) causing increased glycogen and decreased triglyceride in skeletal muscle. PLoS One **2:**e903.
32. **Crawford, S. A., Costford, S.R., Aguer, C., Thomas, S.C., deKemp, R.A., DaSilva, J.N., Lafontaine, D., Kendall, M., Dent, R., Beanlands, R.S.B., McPherson, R., Harper, M.E.** 2010. Naturally occurring R225W mutation of the gene encoding AMP-activated protein kinase (AMPK)[gamma]3 results in increased oxidative capacity and glucose uptake in human primary myotubes. Diabetologia.
33. **Crute, B. E., K. Seefeld, J. Gamble, B. E. Kemp, and L. A. Witters.** 1998. Functional domains of the alpha1 catalytic subunit of the AMP-activated protein kinase. J Biol Chem **273:**35347-54.
34. **Davies, S. P., D. Carling, and D. G. Hardie.** 1989. Tissue distribution of the AMP-activated protein kinase, and lack of activation by cyclic-AMP-dependent protein kinase, studied using a specific and sensitive peptide assay. Eur J Biochem **186:**123-8.
35. **Davies, S. P., N. R. Helps, P. T. Cohen, and D. G. Hardie.** 1995. 5'-AMP inhibits dephosphorylation, as well as promoting phosphorylation, of the AMP-activated protein kinase. Studies using bacterially expressed human protein phosphatase-2C alpha and native bovine protein phosphatase-2AC. FEBS Lett **377:**421-5.
36. **El-Mir, M. Y., V. Nogueira, E. Fontaine, N. Averet, M. Rigoulet, and X. Leverve.** 2000. Dimethylbiguanide inhibits cell respiration via an indirect effect targeted on the respiratory chain complex I. J Biol Chem **275:**223-8.
37. **Ferrer, A., C. Caelles, N. Massot, and F. G. Hegardt.** 1985. Activation of rat liver cytosolic 3-hydroxy-3-methylglutaryl coenzyme A reductase kinase by adenosine 5'-monophosphate. Biochem Biophys Res Commun **132:**497-504.
38. **Folmes, K. D., A. Y. Chan, D. P. Koonen, T. C. Pulinilkunnil, I. Baczko, B. E. Hunter, S. Thorn, M. F. Allard, R. Roberts, M. H. Gollob, P. E. Light, and J. R. Dyck.** 2009. Distinct early signaling events resulting from the expression of the PRKAG2 R302Q mutant of AMPK contribute to increased myocardial glycogen. Circ Cardiovasc Genet **2:**457-66.

39. **Foretz, M., D. Carling, C. Guichard, P. Ferre, and F. Foufelle.** 1998. AMP-activated protein kinase inhibits the glucose-activated expression of fatty acid synthase gene in rat hepatocytes. J Biol Chem **273:**14767-71.
40. **Fryer, L. G., A. Parbu-Patel, and D. Carling.** 2002. The Anti-diabetic drugs rosiglitazone and metformin stimulate AMP-activated protein kinase through distinct signaling pathways. J Biol Chem **277:**25226-32.
41. **Fryer, L. G., A. Parbu-Patel, and D. Carling.** 2002. Protein kinase inhibitors block the stimulation of the AMP-activated protein kinase by 5-amino-4-imidazolecarboxamide riboside. FEBS Lett **531:**189-92.
42. **Fujii, N., M. F. Hirshman, E. M. Kane, R. C. Ho, L. E. Peter, M. M. Seifert, and L. J. Goodyear.** 2005. AMP-activated protein kinase alpha2 activity is not essential for contraction- and hyperosmolarity-induced glucose transport in skeletal muscle. J Biol Chem **280:**39033-41.
43. **Gadalla, A. E., T. Pearson, A. J. Currie, N. Dale, S. A. Hawley, M. Sheehan, W. Hirst, A. D. Michel, A. Randall, D. G. Hardie, and B. G. Frenguelli.** 2004. AICA riboside both activates AMP-activated protein kinase and competes with adenosine for the nucleoside transporter in the CA1 region of the rat hippocampus. J Neurochem **88:**1272-82.
44. **Gaster, M., A. C. Rustan, V. Aas, and H. Beck-Nielsen.** 2004. Reduced lipid oxidation in skeletal muscle from type 2 diabetic subjects may be of genetic origin: evidence from cultured myotubes. Diabetes **53:**542-8.
45. **Geraghty, K. M., S. Chen, J. E. Harthill, A. F. Ibrahim, R. Toth, N. A. Morrice, F. Vandermoere, G. B. Moorhead, D. G. Hardie, and C. MacKintosh.** 2007. Regulation of multisite phosphorylation and 14-3-3 binding of AS160 in response to IGF-1, EGF, PMA and AICAR. Biochem J **407:**231-41.
46. **Gollob, M. H.** 2003. Glycogen storage disease as a unifying mechanism of disease in the PRKAG2 cardiac syndrome. Biochem Soc Trans **31:**228-31.
47. **Gollob, M. H., J. J. Seger, T. N. Gollob, T. Tapscott, O. Gonzales, L. Bachinski, and R. Roberts.** 2001. Novel PRKAG2 mutation responsible for the genetic syndrome of ventricular preexcitation and conduction system disease with childhood onset and absence of cardiac hypertrophy. Circulation **104:**3030-3.
48. **Goransson, O., A. McBride, S. A. Hawley, F. A. Ross, N. Shpiro, M. Foretz, B. Viollet, D. G. Hardie, and K. Sakamoto.** 2007. Mechanism of action of A-769662, a valuable tool for activation of AMP-activated protein kinase. J Biol Chem **282:**32549-60.
49. **Granlund, A., O. Kotova, B. Benziane, D. Galuska, M. Jensen-Waern, A. V. Chibalin, and B. Essen-Gustavsson.** 2010. Effects of exercise on muscle glycogen synthesis signalling and enzyme activities in pigs carrying the PRKAG3 mutation. Exp Physiol **95:**541-9.
50. **Gual, P., T. Gremeaux, T. Gonzalez, Y. Le Marchand-Brustel, and J. F. Tanti.** 2003. MAP kinases and mTOR mediate insulin-induced phosphorylation of insulin receptor substrate-1 on serine residues 307, 612 and 632. Diabetologia **46:**1532-42.
51. **Ha, A. C., J. M. Renaud, R. A. Dekemp, S. Thorn, J. Dasilva, L. Garrard, K. Yoshinaga, A. Abraham, M. S. Green, R. S. Beanlands, and M. H. Gollob.** 2009. In vivo assessment of myocardial glucose uptake by positron emission tomography in adults with the PRKAG2 cardiac syndrome. Circ Cardiovasc Imaging **2:**485-91.

52. **Hamilton, D. N., M. Ellis, K. D. Miller, F. K. McKeith, and D. F. Parrett.** 2000. The effect of the Halothane and Rendement Napole genes on carcass and meat quality characteristics of pigs. J Anim Sci **78:**2862-7.
53. **Hardie, D. G.** 2007. AMP-activated/SNF1 protein kinases: conserved guardians of cellular energy. Nat Rev Mol Cell Biol **8:**774-85.
54. **Hardie, D. G., I. P. Salt, and S. P. Davies.** 2000. Analysis of the role of the AMP-activated protein kinase in the response to cellular stress. Methods Mol Biol **99:**63-74.
55. **Hawley, S. A., J. Boudeau, J. L. Reid, K. J. Mustard, L. Udd, T. P. Makela, D. R. Alessi, and D. G. Hardie.** 2003. Complexes between the LKB1 tumor suppressor, STRAD alpha/beta and MO25 alpha/beta are upstream kinases in the AMP-activated protein kinase cascade. J Biol **2:**28.
56. **Hawley, S. A., M. Davison, A. Woods, S. P. Davies, R. K. Beri, D. Carling, and D. G. Hardie.** 1996. Characterization of the AMP-activated protein kinase kinase from rat liver and identification of threonine 172 as the major site at which it phosphorylates AMP-activated protein kinase. J Biol Chem **271:**27879-87.
57. **Hawley, S. A., M. A. Selbert, E. G. Goldstein, A. M. Edelman, D. Carling, and D. G. Hardie.** 1995. 5'-AMP activates the AMP-activated protein kinase cascade, and Ca2+/calmodulin activates the calmodulin-dependent protein kinase I cascade, via three independent mechanisms. J Biol Chem **270:**27186-91.
58. **Hayashi, T., M. F. Hirshman, N. Fujii, S. A. Habinowski, L. A. Witters, and L. J. Goodyear.** 2000. Metabolic stress and altered glucose transport: activation of AMP-activated protein kinase as a unifying coupling mechanism. Diabetes **49:**527-31.
59. **Hong, S. P., F. C. Leiper, A. Woods, D. Carling, and M. Carlson.** 2003. Activation of yeast Snf1 and mammalian AMP-activated protein kinase by upstream kinases. Proc Natl Acad Sci U S A **100:**8839-43.
60. **Hudson, E. R., D. A. Pan, J. James, J. M. Lucocq, S. A. Hawley, K. A. Green, O. Baba, T. Terashima, and D. G. Hardie.** 2003. A novel domain in AMP-activated protein kinase causes glycogen storage bodies similar to those seen in hereditary cardiac arrhythmias. Curr Biol **13:**861-6.
61. **Iseli, T. J., M. Walter, B. J. van Denderen, F. Katsis, L. A. Witters, B. E. Kemp, B. J. Michell, and D. Stapleton.** 2005. AMP-activated protein kinase beta subunit tethers alpha and gamma subunits via its C-terminal sequence (186-270). J Biol Chem **280:**13395-400.
62. **Iverson, A. J., A. Bianchi, A. C. Nordlund, and L. A. Witters.** 1990. Immunological analysis of acetyl-CoA carboxylase mass, tissue distribution and subunit composition. Biochem J **269:**365-71.
63. **Jaleel, M., F. Villa, M. Deak, R. Toth, A. R. Prescott, D. M. Van Aalten, and D. R. Alessi.** 2006. The ubiquitin-associated domain of AMPK-related kinases regulates conformation and LKB1-mediated phosphorylation and activation. Biochem J **394:**545-55.
64. **Jensen, T. E., A. J. Rose, S. B. Jorgensen, N. Brandt, P. Schjerling, J. F. Wojtaszewski, and E. A. Richter.** 2007. Possible CaMKK-dependent regulation of AMPK phosphorylation and glucose uptake at the onset of mild tetanic skeletal muscle contraction. Am J Physiol Endocrinol Metab **292:**E1308-17.

65. **Jin, X., R. Townley, and L. Shapiro.** 2007. Structural insight into AMPK regulation: ADP comes into play. Structure **15:**1285-95.
66. **Johnson, N. A., S. R. Stannard, and M. W. Thompson.** 2004. Muscle triglyceride and glycogen in endurance exercise: implications for performance. Sports Med **34:**151-64.
67. **Jorgensen, S. B., J. T. Treebak, B. Viollet, P. Schjerling, S. Vaulont, J. F. Wojtaszewski, and E. A. Richter.** 2007. Role of AMPKalpha2 in basal, training-, and AICAR-induced GLUT4, hexokinase II, and mitochondrial protein expression in mouse muscle. Am J Physiol Endocrinol Metab **292:**E331-9.
68. **Jorgensen, S. B., J. F. Wojtaszewski, B. Viollet, F. Andreelli, J. B. Birk, Y. Hellsten, P. Schjerling, S. Vaulont, P. D. Neufer, E. A. Richter, and H. Pilegaard.** 2005. Effects of alpha-AMPK knockout on exercise-induced gene activation in mouse skeletal muscle. FASEB J **19:**1146-8.
69. **Kimura, E., Y. Maeda, T. Arima, Y. Nishida, S. Yamashita, A. Hara, E. Uyama, S. Mita, and M. Uchino.** 2001. Efficient repetitive gene delivery to skeletal muscle using recombinant adenovirus vector containing the Coxsackievirus and adenovirus receptor cDNA. Gene Ther **8:**20-7.
70. **Kimura, N., C. Tokunaga, S. Dalal, C. Richardson, K. Yoshino, K. Hara, B. E. Kemp, L. A. Witters, O. Mimura, and K. Yonezawa.** 2003. A possible linkage between AMP-activated protein kinase (AMPK) and mammalian target of rapamycin (mTOR) signalling pathway. Genes Cells **8:**65-79.
71. **Kishimoto, K., K. Matsumoto, and J. Ninomiya-Tsuji.** 2000. TAK1 mitogen-activated protein kinase kinase kinase is activated by autophosphorylation within its activation loop. J Biol Chem **275:**7359-64.
72. **Kitani, T., S. Okuno, and H. Fujisawa.** 1997. Molecular cloning of Ca2+/calmodulin-dependent protein kinase kinase beta. J Biochem **122:**243-50.
73. **Koay, A., K. A. Rimmer, H. D. Mertens, P. R. Gooley, and D. Stapleton.** 2007. Oligosaccharide recognition and binding to the carbohydrate binding module of AMP-activated protein kinase. FEBS Lett **581:**5055-9.
74. **LeBrasseur, N. K., M. Kelly, T. S. Tsao, S. R. Farmer, A. K. Saha, N. B. Ruderman, and E. Tomas.** 2006. Thiazolidinediones can rapidly activate AMP-activated protein kinase in mammalian tissues. Am J Physiol Endocrinol Metab **291:**E175-81.
75. **Lee, W. J., M. Kim, H. S. Park, H. S. Kim, M. J. Jeon, K. S. Oh, E. H. Koh, J. C. Won, M. S. Kim, G. T. Oh, M. Yoon, K. U. Lee, and J. Y. Park.** 2006. AMPK activation increases fatty acid oxidation in skeletal muscle by activating PPARalpha and PGC-1. Biochem Biophys Res Commun **340:**291-5.
76. **Lessard, S. J., Z. P. Chen, M. J. Watt, M. Hashem, J. J. Reid, M. A. Febbraio, B. E. Kemp, and J. A. Hawley.** 2006. Chronic rosiglitazone treatment restores AMPKalpha2 activity in insulin-resistant rat skeletal muscle. Am J Physiol Endocrinol Metab **290:**E251-7.
77. **Li, J., D. L. Coven, E. J. Miller, X. Hu, M. E. Young, D. Carling, A. J. Sinusas, and L. H. Young.** 2006. Activation of AMPK alpha- and gamma-isoform complexes in the intact ischemic rat heart. Am J Physiol Heart Circ Physiol **291:**H1927-34.

78. **Liu, L., Y. Zhang, N. Chen, X. Shi, B. Tsang, and Y. H. Yu.** 2007. Upregulation of myocellular DGAT1 augments triglyceride synthesis in skeletal muscle and protects against fat-induced insulin resistance. J Clin Invest **117:**1679-89.
79. **Mahlapuu, M., C. Johansson, K. Lindgren, G. Hjalm, B. R. Barnes, A. Krook, J. R. Zierath, L. Andersson, and S. Marklund.** 2004. Expression profiling of the gamma-subunit isoforms of AMP-activated protein kinase suggests a major role for gamma3 in white skeletal muscle. Am J Physiol Endocrinol Metab **286:**E194-200.
80. **Martin, T. L., T. Alquier, K. Asakura, N. Furukawa, F. Preitner, and B. B. Kahn.** 2006. Diet-induced obesity alters AMP kinase activity in hypothalamus and skeletal muscle. J Biol Chem **281:**18933-41.
81. **McBride, A., S. Ghilagaber, A. Nikolaev, and D. G. Hardie.** 2009. The glycogen-binding domain on the AMPK beta subunit allows the kinase to act as a glycogen sensor. Cell Metab **9:**23-34.
82. **Menezes, K. M., H. S. Mok, and M. A. Barry.** 2006. Increased transduction of skeletal muscle cells by fibroblast growth factor-modified adenoviral vectors. Hum Gene Ther **17:**314-20.
83. **Miller, K. D., M. Ellis, F. K. McKeith, B. S. Bidner, and D. J. Meisinger.** 2000. Frequency of the Rendement Napole RN- allele in a population of American Hampshire pigs. J Anim Sci **78:**1811-5.
84. **Minokoshi, Y., T. Alquier, N. Furukawa, Y. B. Kim, A. Lee, B. Xue, J. Mu, F. Foufelle, P. Ferre, M. J. Birnbaum, B. J. Stuck, and B. B. Kahn.** 2004. AMP-kinase regulates food intake by responding to hormonal and nutrient signals in the hypothalamus. Nature **428:**569-74.
85. **Mitchelhill, K. I., B. J. Michell, C. M. House, D. Stapleton, J. Dyck, J. Gamble, C. Ullrich, L. A. Witters, and B. E. Kemp.** 1997. Posttranslational modifications of the 5'-AMP-activated protein kinase beta1 subunit. J Biol Chem **272:**24475-9.
86. **Mitchelhill, K. I., D. Stapleton, G. Gao, C. House, B. Michell, F. Katsis, L. A. Witters, and B. E. Kemp.** 1994. Mammalian AMP-activated protein kinase shares structural and functional homology with the catalytic domain of yeast Snf1 protein kinase. J Biol Chem **269:**2361-4.
87. **Momcilovic, M., S. P. Hong, and M. Carlson.** 2006. Mammalian TAK1 activates Snf1 protein kinase in yeast and phosphorylates AMP-activated protein kinase in vitro. J Biol Chem **281:**25336-43.
88. **Momcilovic, M., S. H. Iram, Y. Liu, and M. Carlson.** 2008. Roles of the glycogen-binding domain and Snf4 in glucose inhibition of SNF1 protein kinase. J Biol Chem **283:**19521-9.
89. **Munday, M. R.** 2002. Regulation of mammalian acetyl-CoA carboxylase. Biochem Soc Trans **30:**1059-64.
90. **Munday, M. R., D. G. Campbell, D. Carling, and D. G. Hardie.** 1988. Identification by amino acid sequencing of three major regulatory phosphorylation sites on rat acetyl-CoA carboxylase. Eur J Biochem **175:**331-8.
91. **Nagata, D., and Y. Hirata.** 2010. The role of AMP-activated protein kinase in the cardiovascular system. Hypertens Res **33:**22-8.
92. **Nayak, V., K. Zhao, A. Wyce, M. F. Schwartz, W. S. Lo, S. L. Berger, and R. Marmorstein.** 2006. Structure and dimerization of the kinase domain from yeast Snf1, a member of the Snf1/AMPK protein family. Structure **14:**477-85.

93. **Nordstrom, J. L., V. W. Rodwell, and J. J. Mitschelen.** 1977. Interconversion of active and inactive forms of rat liver hydroxymethylglutaryl-CoA reductase. J Biol Chem **252:**8924-34.
94. **Ofir, M., E. Hochhauser, B. A. Vidne, D. Freimark, and M. Arad.** 2007. [AMP-activated protein kinase: how a mistake in energy gauge causes glycogen storage]. Harefuah **146:**770-5, 813-4.
95. **Olsson, V., A. Solyakov, K. Skog, K. Lundstrom, and M. Jagerstad.** 2002. Natural variations of precursors in pig meat affect the yield of heterocyclic amines--effects of RN genotype, feeding regime, and sex. J Agric Food Chem **50:**2962-9.
96. **Ono, K., T. Ohtomo, S. Sato, Y. Sugamata, M. Suzuki, N. Hisamoto, J. Ninomiya-Tsuji, M. Tsuchiya, and K. Matsumoto.** 2001. An evolutionarily conserved motif in the TAB1 C-terminal region is necessary for interaction with and activation of TAK1 MAPKKK. J Biol Chem **276:**24396-400.
97. **Owen, M. R., E. Doran, and A. P. Halestrap.** 2000. Evidence that metformin exerts its anti-diabetic effects through inhibition of complex 1 of the mitochondrial respiratory chain. Biochem J **348 Pt 3:**607-14.
98. **Pang, T., B. Xiong, J. Y. Li, B. Y. Qiu, G. Z. Jin, J. K. Shen, and J. Li.** 2007. Conserved alpha-helix acts as autoinhibitory sequence in AMP-activated protein kinase alpha subunits. J Biol Chem **282:**495-506.
99. **Park, S. H., S. R. Gammon, J. D. Knippers, S. R. Paulsen, D. S. Rubink, and W. W. Winder.** 2002. Phosphorylation-activity relationships of AMPK and acetyl-CoA carboxylase in muscle. J Appl Physiol **92:**2475-82.
100. **Parker, G. J., A. Koay, R. Gilbert-Wilson, L. J. Waddington, and D. Stapleton.** 2007. AMP-activated protein kinase does not associate with glycogen alpha-particles from rat liver. Biochem Biophys Res Commun **362:**811-5.
101. **Polekhina, G., A. Gupta, B. J. Michell, B. van Denderen, S. Murthy, S. C. Feil, I. G. Jennings, D. J. Campbell, L. A. Witters, M. W. Parker, B. E. Kemp, and D. Stapleton.** 2003. AMPK beta subunit targets metabolic stress sensing to glycogen. Curr Biol **13:**867-71.
102. **Polekhina, G., A. Gupta, B. J. van Denderen, S. C. Feil, B. E. Kemp, D. Stapleton, and M. W. Parker.** 2005. Structural basis for glycogen recognition by AMP-activated protein kinase. Structure **13:**1453-62.
103. **Polge, C., and M. Thomas.** 2007. SNF1/AMPK/SnRK1 kinases, global regulators at the heart of energy control? Trends Plant Sci **12:**20-8.
104. **Qiao, L., C. Zou, P. Shao, J. Schaack, P. F. Johnson, and J. Shao.** 2008. Transcriptional regulation of fatty acid translocase/CD36 expression by CCAAT/enhancer-binding protein alpha. J Biol Chem **283:**8788-95.
105. **Reiter, A. K., D. R. Bolster, S. J. Crozier, S. R. Kimball, and L. S. Jefferson.** 2005. Repression of protein synthesis and mTOR signaling in rat liver mediated by the AMPK activator aminoimidazole carboxamide ribonucleoside. Am J Physiol Endocrinol Metab **288:**E980-8.
106. **Rolfe, D. F., and G. C. Brown.** 1997. Cellular energy utilization and molecular origin of standard metabolic rate in mammals. Physiol Rev **77:**731-58.
107. **Rudolph, M. J., G. A. Amodeo, Y. Bai, and L. Tong.** 2005. Crystal structure of the protein kinase domain of yeast AMP-activated protein kinase Snf1. Biochem Biophys Res Commun **337:**1224-8.

108. **Russell, R. R., 3rd, R. Bergeron, G. I. Shulman, and L. H. Young.** 1999. Translocation of myocardial GLUT-4 and increased glucose uptake through activation of AMPK by AICAR. Am J Physiol **277:**H643-9.
109. **Sabina, R. L., D. Patterson, and E. W. Holmes.** 1985. 5-Amino-4-imidazolecarboxamide riboside (Z-riboside) metabolism in eukaryotic cells. J Biol Chem **260:**6107-14.
110. **Sakamoto, K., O. Goransson, D. G. Hardie, and D. R. Alessi.** 2004. Activity of LKB1 and AMPK-related kinases in skeletal muscle: effects of contraction, phenformin, and AICAR. Am J Physiol Endocrinol Metab **287:**E310-7.
111. **Sakurai, H., H. Miyoshi, J. Mizukami, and T. Sugita.** 2000. Phosphorylation-dependent activation of TAK1 mitogen-activated protein kinase kinase kinase by TAB1. FEBS Lett **474:**141-5.
112. **Salt, I., J. W. Celler, S. A. Hawley, A. Prescott, A. Woods, D. Carling, and D. G. Hardie.** 1998. AMP-activated protein kinase: greater AMP dependence, and preferential nuclear localization, of complexes containing the alpha2 isoform. Biochem J **334 (Pt 1):**177-87.
113. **Sanders, M. J., P. O. Grondin, B. D. Hegarty, M. A. Snowden, and D. Carling.** 2007. Investigating the mechanism for AMP activation of the AMP-activated protein kinase cascade. Biochem J **403:**139-48.
114. **Sano, H., S. Kane, E. Sano, C. P. Miinea, J. M. Asara, W. S. Lane, C. W. Garner, and G. E. Lienhard.** 2003. Insulin-stimulated phosphorylation of a Rab GTPase-activating protein regulates GLUT4 translocation. J Biol Chem **278:**14599-602.
115. **Savage, D. B., C. S. Choi, V. T. Samuel, Z. X. Liu, D. Zhang, A. Wang, X. M. Zhang, G. W. Cline, X. X. Yu, J. G. Geisler, S. Bhanot, B. P. Monia, and G. I. Shulman.** 2006. Reversal of diet-induced hepatic steatosis and hepatic insulin resistance by antisense oligonucleotide inhibitors of acetyl-CoA carboxylases 1 and 2. J Clin Invest **116:**817-24.
116. **Scott, J. W., S. A. Hawley, K. A. Green, M. Anis, G. Stewart, G. A. Scullion, D. G. Norman, and D. G. Hardie.** 2004. CBS domains form energy-sensing modules whose binding of adenosine ligands is disrupted by disease mutations. J Clin Invest **113:**274-84.
117. **Scott, J. W., F. A. Ross, J. K. Liu, and D. G. Hardie.** 2007. Regulation of AMP-activated protein kinase by a pseudosubstrate sequence on the gamma subunit. EMBO J **26:**806-15.
118. **Shibuya, H., K. Yamaguchi, K. Shirakabe, A. Tonegawa, Y. Gotoh, N. Ueno, K. Irie, E. Nishida, and K. Matsumoto.** 1996. TAB1: an activator of the TAK1 MAPKKK in TGF-beta signal transduction. Science **272:**1179-82.
119. **Sidhu, J. S., Y. S. Rajawat, T. G. Rami, M. H. Gollob, Z. Wang, R. Yuan, A. J. Marian, F. J. DeMayo, D. Weilbacher, G. E. Taffet, J. K. Davies, D. Carling, D. S. Khoury, and R. Roberts.** 2005. Transgenic mouse model of ventricular preexcitation and atrioventricular reentrant tachycardia induced by an AMP-activated protein kinase loss-of-function mutation responsible for Wolff-Parkinson-White syndrome. Circulation **111:**21-9.

120. **Smith, D. P., J. Spicer, A. Smith, S. Swift, and A. Ashworth.** 1999. The mouse Peutz-Jeghers syndrome gene Lkb1 encodes a nuclear protein kinase. Hum Mol Genet **8:**1479-85.
121. **Srivastava, A. K., X. Qin, N. Wedhas, M. Arnush, T. A. Linkhart, R. B. Chadwick, and A. Kumar.** 2007. Tumor necrosis factor-alpha augments matrix metalloproteinase-9 production in skeletal muscle cells through the activation of transforming growth factor-beta-activated kinase 1 (TAK1)-dependent signaling pathway. J Biol Chem **282:**35113-24.
122. **Sriwijitkamol, A., J. L. Ivy, C. Christ-Roberts, R. A. DeFronzo, L. J. Mandarino, and N. Musi.** 2006. LKB1-AMPK signaling in muscle from obese insulin-resistant Zucker rats and effects of training. Am J Physiol Endocrinol Metab **290:**E925-32.
123. **Stapleton, D., K. I. Mitchelhill, G. Gao, J. Widmer, B. J. Michell, T. Teh, C. M. House, C. S. Fernandez, T. Cox, L. A. Witters, and B. E. Kemp.** 1996. Mammalian AMP-activated protein kinase subfamily. J Biol Chem **271:**611-4.
124. **Staron, R. S., F. C. Hagerman, R. S. Hikida, T. F. Murray, D. P. Hostler, M. T. Crill, K. E. Ragg, and K. Toma.** 2000. Fiber type composition of the vastus lateralis muscle of young men and women. J Histochem Cytochem **48:**623-9.
125. **Steinberg, G. R., and B. E. Kemp.** 2009. AMPK in Health and Disease. Physiol Rev **89:**1025-78.
126. **Steinberg, G. R., B. J. Michell, B. J. van Denderen, M. J. Watt, A. L. Carey, B. C. Fam, S. Andrikopoulos, J. Proietto, C. Z. Gorgun, D. Carling, G. S. Hotamisligil, M. A. Febbraio, T. W. Kay, and B. E. Kemp.** 2006. Tumor necrosis factor alpha-induced skeletal muscle insulin resistance involves suppression of AMP-kinase signaling. Cell Metab **4:**465-74.
127. **Steinberg, G. R., A. C. Smith, B. J. Van Denderen, Z. Chen, S. Murthy, D. J. Campbell, G. J. Heigenhauser, D. J. Dyck, and B. E. Kemp.** 2004. AMP-activated protein kinase is not down-regulated in human skeletal muscle of obese females. J Clin Endocrinol Metab **89:**4575-80.
128. **Suter, M., U. Riek, R. Tuerk, U. Schlattner, T. Wallimann, and D. Neumann.** 2006. Dissecting the role of 5'-AMP for allosteric stimulation, activation, and deactivation of AMP-activated protein kinase. J Biol Chem **281:**32207-16.
129. **Taylor, E. B., D. An, H. F. Kramer, H. Yu, N. L. Fujii, K. S. Roeckl, N. Bowles, M. F. Hirshman, J. Xie, E. P. Feener, and L. J. Goodyear.** 2008. Discovery of TBC1D1 as an insulin-, AICAR-, and contraction-stimulated signaling nexus in mouse skeletal muscle. J Biol Chem **283:**9787-96.
130. **Tokumitsu, H., M. Iwabu, Y. Ishikawa, and R. Kobayashi.** 2001. Differential regulatory mechanism of Ca2+/calmodulin-dependent protein kinase kinase isoforms. Biochemistry **40:**13925-32.
131. **Townley, R., and L. Shapiro.** 2007. Crystal structures of the adenylate sensor from fission yeast AMP-activated protein kinase. Science **315:**1726-9.
132. **Ukropcova, B., M. McNeil, O. Sereda, L. de Jonge, H. Xie, G. A. Bray, and S. R. Smith.** 2005. Dynamic changes in fat oxidation in human primary myocytes mirror metabolic characteristics of the donor. J Clin Invest **115:**1934-41.
133. **Venditti, P., A. Bari, L. Di Stefano, A. Cardone, F. Della Ragione, M. D'Esposito, and S. Di Meo.** 2009. Involvement of PGC-1, NRF-1, and NRF-2 in

metabolic response by rat liver to hormonal and environmental signals. Mol Cell Endocrinol **305:**22-9.

134. **Vercauteren, K., N. Gleyzer, and R. C. Scarpulla.** 2008. PGC-1-related coactivator complexes with HCF-1 and NRF-2beta in mediating NRF-2(GABP)-dependent respiratory gene expression. J Biol Chem **283:**12102-11.
135. **Wang, M. Y., and R. H. Unger.** 2005. Role of PP2C in cardiac lipid accumulation in obese rodents and its prevention by troglitazone. Am J Physiol Endocrinol Metab **288:**E216-21.
136. **Watt, M. J., N. Dzamko, W. G. Thomas, S. Rose-John, M. Ernst, D. Carling, B. E. Kemp, M. A. Febbraio, and G. R. Steinberg.** 2006. CNTF reverses obesity-induced insulin resistance by activating skeletal muscle AMPK. Nat Med **12:**541-8.
137. **Watt, M. J., G. R. Steinberg, S. Chan, A. Garnham, B. E. Kemp, and M. A. Febbraio.** 2004. Beta-adrenergic stimulation of skeletal muscle HSL can be overridden by AMPK signaling. FASEB J **18:**1445-6.
138. **Westerman, A. M., M. M. Entius, P. P. Boor, R. Koole, E. de Baar, G. J. Offerhaus, J. Lubinski, D. Lindhout, D. J. Halley, F. W. de Rooij, and J. H. Wilson.** 1999. Novel mutations in the LKB1/STK11 gene in Dutch Peutz-Jeghers families. Hum Mutat **13:**476-81.
139. **WHO** 2010 2006, posting date. WHO | Obesity and Overweight Fact Sheet. [Online.]
140. **Williamson, D. L., D. R. Bolster, S. R. Kimball, and L. S. Jefferson.** 2006. Time course changes in signaling pathways and protein synthesis in C2C12 myotubes following AMPK activation by AICAR. Am J Physiol Endocrinol Metab **291:**E80-9.
141. **Wilson, W. A., S. A. Hawley, and D. G. Hardie.** 1996. Glucose repression/derepression in budding yeast: SNF1 protein kinase is activated by phosphorylation under derepressing conditions, and this correlates with a high AMP:ATP ratio. Curr Biol **6:**1426-34.
142. **Winder, W. W., B. F. Holmes, D. S. Rubink, E. B. Jensen, M. Chen, and J. O. Holloszy.** 2000. Activation of AMP-activated protein kinase increases mitochondrial enzymes in skeletal muscle. J Appl Physiol **88:**2219-26.
143. **Witczak, C. A., N. Fujii, M. F. Hirshman, and L. J. Goodyear.** 2007. Ca2+/calmodulin-dependent protein kinase kinase-alpha regulates skeletal muscle glucose uptake independent of AMP-activated protein kinase and Akt activation. Diabetes **56:**1403-9.
144. **Witczak, C. A., C. G. Sharoff, and L. J. Goodyear.** 2008. AMP-activated protein kinase in skeletal muscle: from structure and localization to its role as a master regulator of cellular metabolism. Cell Mol Life Sci **65:**3737-55.
145. **Wojtaszewski, J. F., S. B. Jorgensen, Y. Hellsten, D. G. Hardie, and E. A. Richter.** 2002. Glycogen-dependent effects of 5-aminoimidazole-4-carboxamide (AICA)-riboside on AMP-activated protein kinase and glycogen synthase activities in rat skeletal muscle. Diabetes **51:**284-92.
146. **Woods, A., S. R. Johnstone, K. Dickerson, F. C. Leiper, L. G. Fryer, D. Neumann, U. Schlattner, T. Wallimann, M. Carlson, and D. Carling.** 2003. LKB1 is the upstream kinase in the AMP-activated protein kinase cascade. Curr Biol **13:**2004-8.

147. **Woods, A., M. R. Munday, J. Scott, X. Yang, M. Carlson, and D. Carling.** 1994. Yeast SNF1 is functionally related to mammalian AMP-activated protein kinase and regulates acetyl-CoA carboxylase in vivo. J Biol Chem **269:**19509-15.
148. **Xiao, B., R. Heath, P. Saiu, F. C. Leiper, P. Leone, C. Jing, P. A. Walker, L. Haire, J. F. Eccleston, C. T. Davis, S. R. Martin, D. Carling, and S. J. Gamblin.** 2007. Structural basis for AMP binding to mammalian AMP-activated protein kinase. Nature **449:**496-500.
149. **Xie, M., D. Zhang, J. R. Dyck, Y. Li, H. Zhang, M. Morishima, D. L. Mann, G. E. Taffet, A. Baldini, D. S. Khoury, and M. D. Schneider.** 2006. A pivotal role for endogenous TGF-beta-activated kinase-1 in the LKB1/AMP-activated protein kinase energy-sensor pathway. Proc Natl Acad Sci U S A **103:**17378-83.
150. **Yeh, L. A., K. H. Lee, and K. H. Kim.** 1980. Regulation of rat liver acetyl-CoA carboxylase. Regulation of phosphorylation and inactivation of acetyl-CoA carboxylase by the adenylate energy charge. J Biol Chem **255:**2308-14.
151. **Yu, H., N. Fujii, M. F. Hirshman, J. M. Pomerleau, and L. J. Goodyear.** 2004. Cloning and characterization of mouse 5'-AMP-activated protein kinase gamma3 subunit. Am J Physiol Cell Physiol **286:**C283-92.
152. **Zhou, G., R. Myers, Y. Li, Y. Chen, X. Shen, J. Fenyk-Melody, M. Wu, J. Ventre, T. Doebber, N. Fujii, N. Musi, M. F. Hirshman, L. J. Goodyear, and D. E. Moller.** 2001. Role of AMP-activated protein kinase in mechanism of metformin action. J Clin Invest **108:**1167-74.

Contributions of Collaborators

We would like to acknowledge our collaborators for their assistance in this project. Dr. Michael Gollob, of the University of Ottawa Heart Institute, recruited all of the R302Q variant subjects. Dr. Robert Dent, of the Ottawa Hospital Weight Management Clinic, and Dr. Ruth McPherson, of the University of Ottawa Heart Institute, performed the skeletal muscle biopsies on all recruited subjects. Dr. Ruth McPherson also retained skeletal muscle samples obtained during the biopsy for later mRNA analysis.

Curriculum Vitae
Cynthia Moffat

EDUCATION
University of Toronto, B.Sc., Honours Biochemistry, 2007
University of Ottawa, M.Sc., Biochemistry, 2010

EXPERIENCE
Dr. Mary Ellen Harper, University of Ottawa From: 09/2007 To: 05/2010
Master's Student
Investigating the impact of the AMPK γ2 R302Q mutation on human skeletal muscle metabolism. Utilizing primary human myoblast samples collected from an affected patient population to analyze the impact of the mutation on cell signalling and fuel storage, as well as transgenically expressing the mutation in the C2C12 muscle cell line using an adenoviral vector.

Dr. Michael McBurney, Ottawa Regional Cancer Centre From: 04/2006 To: 08/2006
Summer Student
Investigating the role of SirT1 on cell signaling pathways. Using immortalized MEFs from SirT1 KO and WT mice, determined the phenotypic effect on mitochondrial dynamics and membrane potential. Isolated mitochondria from the two mouse lines to analyze direct effects on mitochondrial metabolism and efficiency.

Dr. Mary Ellen Harper, University of Ottawa From: 05/2005 To: 08/2005
Summer Student
Optimized a Reactive Oxygen Species detection assay using isolated mitochondria and fluorometric indicators. Collaborated with Dr. David Parks to determine the mitochondrial efficiency of DJ-1 knockout mice against matched wild types.

Dr. Mary Ellen Harper, University of Ottawa From: 05/2004 To: 08/2004
Summer Student
Determined differences between "diet sensitive" and "diet resistant" mice by measuring differences in carbohydrate fuel storage, and characteristics of their tissues.

VOLUNTEER WORK
Scouts Canada From: 08/2008 To: Present
Assisting in Catering and Food services with the Camp Opemikon Rover Troupe.

MS Society of Canada From: 08/2008 To: 08/2009
Participated in annual 190km bikeathon to raise funds for MS research in Canada.

Let's Talk Science From: 09/2008 To: 05/2009
Ran educational in-class sessions, or assisting and judging in science fairs at local schools.

House Manager at Ottawa Fringe Festival From: 08/2002 To: 08/2004
Assisted and supervised Box Office sales. Managed till and trained new volunteers.

AWARDS
Dean's List 2004
Regent's In Course Scholarship 2004

TRAINING
Advanced Laboratory Course in Biochemistry, University of Toronto
From: 2006-2007
- Protein Purification
- Immunochemistry
- Enzyme Kinetics
- X-Ray Crystallography
- DNA Recombination
- ELISA

Summer Studentships, University of Ottawa
From: 2004-2007
- Western Blotting
- Small Animal Dissection
- Mitochondrial Isolation
- Fluorimetric Assays
- Flow Cytometry

Master's Program, University of Ottawa
From: 2007-2010
- Satellite Cell Isolation from Biopsy
- Cardiomyocyte Isolation from Neonatal Mice.
- Cell Culture (Human Primary Myoblasts, HEK 293T, C2C12, MEF, Primary Mouse Cardiomyocytes)
- Immunoprecipitation
- Kinase Assays
- Radioassays

PUBLICATIONS
SirT1 Regulates Energy Metabolism and Response to Caloric Restriction in Mice. Gino Boily, Erin L. Seifert, Lisa Bevilacqua, Xiao Hong He, Guillaume Sabourin, Carmen Estey, **Cynthia Moffat**, Sean Crawford, Sarah Saliba, Karen Jardine, Jian Xuan, Meredith Evans, Mary-Ellen Harper, Michael W. McBurney. March 2008. PLoS One.

POSTERS AND ABSTRACTS
Whole-body Lipogenesis During Refeeding is Increased in UCP3 Knockout Mice & Decreased in UCP3 Transgenic Mice. Martin Gerrits, **Cynthia Moffat**, Mahmoud Salkhordeh, Mary Ellen Harper. Canadian Federation of Biological Sciences (CFBS): Guelph Ontario. June 2005

The AMPK γ2 R302Q Mutation and Its Impact on Human Skeletal Muscle Metabolism. **Cynthia Moffat**, Robert Dent, Ruth McPherson, Mike Gollob, Mary Ellen Harper. University of Ottawa Graduate Poster Day. May 2008

COMMITTEES AND ORGANIZATIONS
MFI Student Symposium Organizational Committee – Logistics
From: 2007 To: 2008
MFI Student Symposium Organizational Committee - Co-Chair of Social Committee
From: 2008 To: 2009

SKILLS
Well versed with Microsoft Office programs including Word, Excel and Powerpoint. Adept at GraphPad Prism graphing software, and Image J open source image analysis tool.